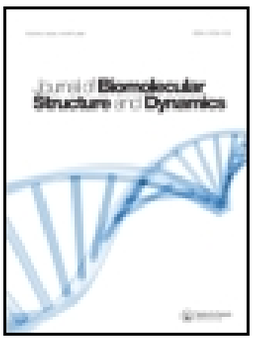

Taylor & Francis
Taylor & Francis Group

Journal of Biomolecular Structure and Dynamics

ISSN: 0739-1102 (Print) 1538-0254 (Online) Journal homepage: http://www.tandfonline.com/loi/tbsd20

Orthosteric and benzodiazepine cavities of the $\alpha_1\beta_2\gamma_2$ $GABA_A$ receptor: Insights from experimentally-validated in silico methods.

María Julia Amundarain, Juan Francisco Viso, Fernando Zamarreño, Alejandro Giorgetti & Marcelo Costabel

To cite this article: María Julia Amundarain, Juan Francisco Viso, Fernando Zamarreño, Alejandro Giorgetti & Marcelo Costabel (2018): Orthosteric and benzodiazepine cavities of the $\alpha_1\beta_2\gamma_2$ $GABA_A$ receptor: Insights from experimentally-validated in silico methods., Journal of Biomolecular Structure and Dynamics, DOI: 10.1080/07391102.2018.1462733

To link to this article: https://doi.org/10.1080/07391102.2018.1462733

Publisher: Taylor & Francis

Journal: *Journal of Biomolecular Structure and Dynamics*

DOI: http://doi.org/10.1080/07391102.2018.1462733

Orthosteric and benzodiazepine cavities of the $\alpha_1\beta_2\gamma_2$ $GABA_A$ receptor: Insights from experimentally-validated *in silico* methods.

María Julia Amundarain (1), Juan Francisco Viso (1), Fernando Zamarreño (1), Alejandro Giorgetti (2)(3)*, Marcelo Costabel (1)*.

(1) Instituto de Física del Sur (IFISUR), Departamento de Física, Universidad Nacional del Sur (UNS), CONICET, Bahía Blanca, Argentina.

(2) Department of Biotechnology, Faculty of Mathematical, Physical and Natural Sciences, University of Verona, Verona, Italy.

(3) Computational Biomedicine, Institute for Advanced Simulation IAS-5 and Computational Biomedicine, Institute of Neuroscience and Medicine INM-9, Forschungszentrum Jülich, Germany.

* Corresponding Authors:

E-mail: alejandro.giorgetti@univr.it. Telephone: +39-045-8027905 Address: Strada Le Grazie N. 15, Ca' Vignal, 37134, Verona, Italy.

E-mail: costabel@criba.edu.ar. Telephone: +54-291- 4595101 Ext 2805. Address: Av. L. N. Alem 1253, B8000CPB, Bahía Blanca, Argentina

Orthosteric and benzodiazepine cavities of the $\alpha_1\beta_2\gamma_2$ $GABA_A$ receptor: Insights from experimentally-validated *in silico* methods.

γ-aminobutyric acid type A ($GABA_A$) receptors mediate fast synaptic inhibition in the central nervous system of mammals. They are modulated via several sites by numerous compounds, which include GABA, benzodiazepines, ethanol, neurosteroids and anaesthetics among others. Due to their potential as targets of novel drugs, a detailed knowledge of their structure-function relationships is needed.

Here, we present the model of the $\alpha_1\beta_2\gamma_2$ subtype $GABA_A$ receptor in the APO state and in complex with selected ligands, including agonists, antagonists and allosteric modulators. The model is based on the crystallographic structure of the human β_3 homopentamer $GABA_A$ receptor. The complexes were refined using atomistic molecular dynamics simulations. This allowed a broad description of the binding modes and the detection of important interactions in agreement with experimental information.

From the best of our knowledge, this is the only model of the $\alpha_1\beta_2\gamma_2$ $GABA_A$ receptor that represents altogether the desensitized state of the channel and comprehensively describes the interactions of ligands of the orthosteric and benzodiazepines binding sites in agreement with the available experimental data. Furthermore, it is able to explain small differences regarding the binding of a variety of chemically divergent ligands. Finally, this new model may pave the way for the design of focused experimental studies that will allow a deeper description of the receptor.

Keywords: GABAAR; Benzodiazepines; Homology Modelling; Docking; Molecular Dynamics.

List of Abbreviations

GABA	Gamma-Aminobutyric acid
GABAARs	Gamma-Aminobutyric Acid type A receptors
CNS	Central Nervous System
ECD	Extracellular domain

TMD	Transmembrane domain
ELIC	Erwinia ligand-gated ion channel
GLIC	Gloeobacter ligand-gated ion channel
AChBP	Acetylcholine Binding Protein
BZDs	Benzodiazepines
i-BZDs	Imidazo-Benzodiazepines
MD	Molecular Dynamics
SCAM	Substituted cysteine accessibility method
POPC	1-palmitoyl-2-oleoyl-phophatidylcholine

Introduction

Gamma-Aminobutyric Acid type A receptors ($GABA_A$Rs) are the main inhibitory neurotransmitter receptors in the mammalian central nervous system (Young & Chu, 1990). They are members of the Cys-Loop family of Pentameric Ligand Gated Ion Channels (PLGICs), along with the cation-selective, excitatory, nicotinic-acetylcholine receptors and serotonin receptors; and with the anion-selective, inhibitory, $GABA_C$ and Glycine receptors (Ortells & Lunt, 1995).

$GABA_A$Rs are well characterized as pharmaceutical targets, and thus should be exhaustively studied: they have binding sites for a variety of ligands such as GABA, benzodiazepines, barbiturates, β-carbolines and neurosteroids among others (Werner Sieghart, 1995). In addition, they are involved in a myriad of neurological processes related not only to the regulation of inhibition in the CNS but also to the variability of GABAergic signals (Rudolph, Crestani, Hanns, & Rudolph, 2001; Vogt, 2015). Their correct functioning is extremely important for the health of humans; dysfunctional $GABA_A$Rs have been related to anxiety, sleep disorders, epilepsy, alcohol dependence, among other affections (Collins et al., 2006; Crestani et al., 1999; Jones-Davis & Macdonald, 2003; Mukherjee, Das, Vaidyanathan, & Vasudevan, 2008; Nutt & Malizia, 2001; Yee et al., 2005) .

$GABA_A$ receptors are integral-transmembrane proteins formed by a pseudosymetrical arrangement of five subunits, which form a chloride-conducting pore in its centre. There is a wealth of $GABA_A$ receptor subtypes which display distinct regional, cellular and subcellular expression patterns and contribute distinctly to several functions (W Sieghart & Sperk, 2002). This diversity is due to the assembly of different combinations of the subunits isoforms; so far 19 of them are known: α1–6, β1–3, γ1–3,δ,ε,θ,π, ρ1–3 (Simon, Wakimoto, Fujita, Lalande, & Barnard, 2004). The most abundant isoform in the human CNS is the $\alpha_1\beta_2\gamma_2$ subtype; which, if viewed from the extracellular side, displays its subunits sequentially ordered as α_1:β_2:α_1:β_2:γ_2 (anticlockwise)(Figure 1) (Tretter, Ehya, Fuchs, & Sieghart, 1997).

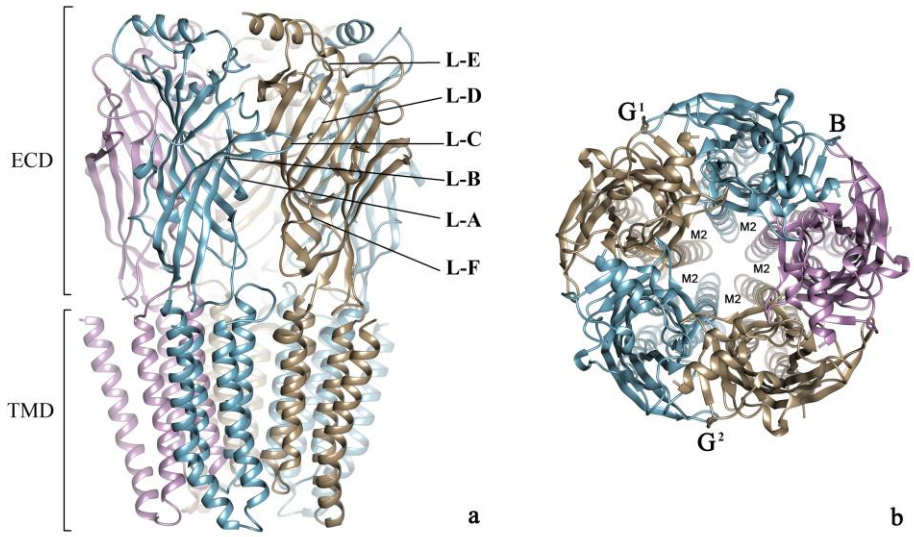

Figure 1. Views of a GABAA receptor depicted with ribbons and coloured according to the subunits. α1 in light blue, β2 in tan and γ2 in lilac. a. Side view of the receptor. The extracellular and transmembrane domains are marked, as well as the loops involved in ligand binding. b. Front view of the receptor from the extracellular side; the binding sites of GABA (orthosteric cavity) are indicated with G1 and G2 and the Benzodiazepines high affinity binding cavity is indicated with B. The M2 helices are the ones that line the pore.

These receptors are generally divided into three distinct domains (Smith & Olsen, 1995): the extracellular, the transmembrane and the intracellular. The extracellular domain (ECD) is also known as the ligand binding domain because it hosts the orthosteric and benzodiazepines binding cavities. It is formed by ten beta strands and two alpha helices. The transmembrane domain (TMD), which is formed by four alpha helices, controls the opening and closing of the channel pore through the movement of the inner (M2) helices. It also contains the binding cavities for other ligands, such as neurosteroids, ethanol and anaesthetics. The intracellular (IC) loop has not been completely solved experimentally, although it is known to be partially formed by an alpha helix. This domain helps modulate the flux of ions and the function of the channel by different mechanisms such as tyrosine phosphorylation (Kittler & Moss, 2003; Moss, Gorrie, Amato, & Smart, 1995) and the interaction with other proteins.

In this work, and due to their pharmaceutical relevance, we focused on the characterization of the orthosteric and high affinity benzodiazepines binding sites. These cavities are homologous and they are located between different pairs of subunits. They are both formed by loops A, B and C from the principal subunits and loops D, E and F of the respective complementary subunits (Figure 1.a). Different roles have been assigned to these loops in the binding of ligands and in allosteric interaction between sites, as well as in transmission of the signal in channel gating. Studies of the binding cavities of Cys-loop

receptors and AChBPs with known structures (Calimet et al., 2013; Puthenkalam et al., 2016) have shown that they undergo conformational changes after the binding of the ligands. In particular, loop C has been shown to be very mobile, closing itself after agonist binding and adopting a more open conformation if the ligand is an antagonist (Puthenkalam et al., 2016). These cavities are allosterically and bi-directionally related: modulators that bind to the Benzodiazepines cavity modify the conformation of the orthosteric binding sites (Changeux & Edelstein, 1998) and it was also demonstrated that the binding of GABA and its activation of the receptor cause structural rearrangements in the benzodiazepines site (Teissére & Czajkowski, 2001). While the binding of agonists of the benzodiazepines binding site is positively coupled to the binding of GABA, imidazo-benzodiazepines are negatively coupled, i.e. these modulators stabilize different conformations of the receptor (Teissére & Czajkowski, 2001).

There are two orthosteric binding sites, which are located in the ECD between the principal face of a β-subunit and the complementary face of an α-subunit (β+/α-) (Figure 1.b). While site G^1 is surrounded by a γ- and a β-subunit, site G^2 is flanked by an α- and a γ-subunit. Different compounds are known to bind to these cavities; those include the agonist GABA, muscimol, bicuculline and gabazine (SR-95531), (Figure 2). On the other hand, the allosteric high affinity benzodiazepines' binding pocket lies between the principal face of an α-subunit and the complementary face of the γ-subunit (α+/γ-)(Sigel & Buhr, 1997). The different compounds that bind to this site exhibit specific effects and binding affinities. Classic benzodiazepines (BZDs), such as diazepam, clonazepam, flurazepam and flunitrazepam, display a common 1,4-benzodiazepine nucleus with a 5-phenyl substituent (Sternbach, 1979); imidazo-benzodiazepines (i-BZDs), such as flumazenil (Ro15-1788) and Ro15-4513, lack the 5-phenyl substituent but possess instead an imidazole ring substituted at positions 1 and 2 of the diazepine nucleus. Furthermore, there are other non-benzodiazepine ligands of this site, which include the imidazopyridine Zolpidem and the cyclopyrrolone Eszopiclone (S-zopiclone) (Figure 3).

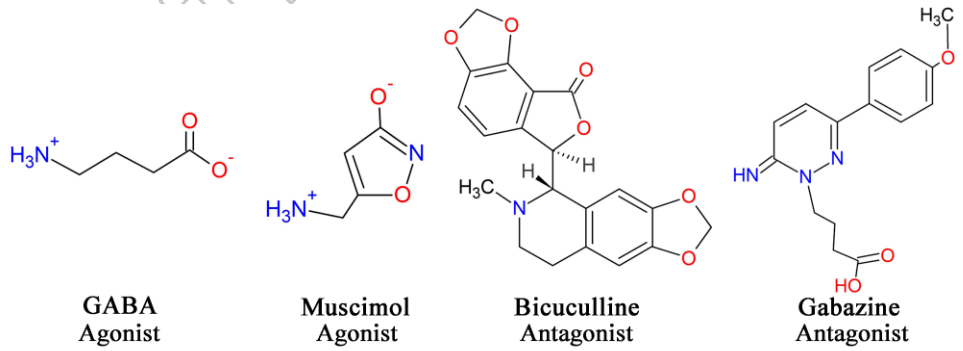

Figure 2. 2D chemical structures of the ligands of the orthosteric cavity employed in this work: GABA, Muscimol, Bicuculline and Gabazine.

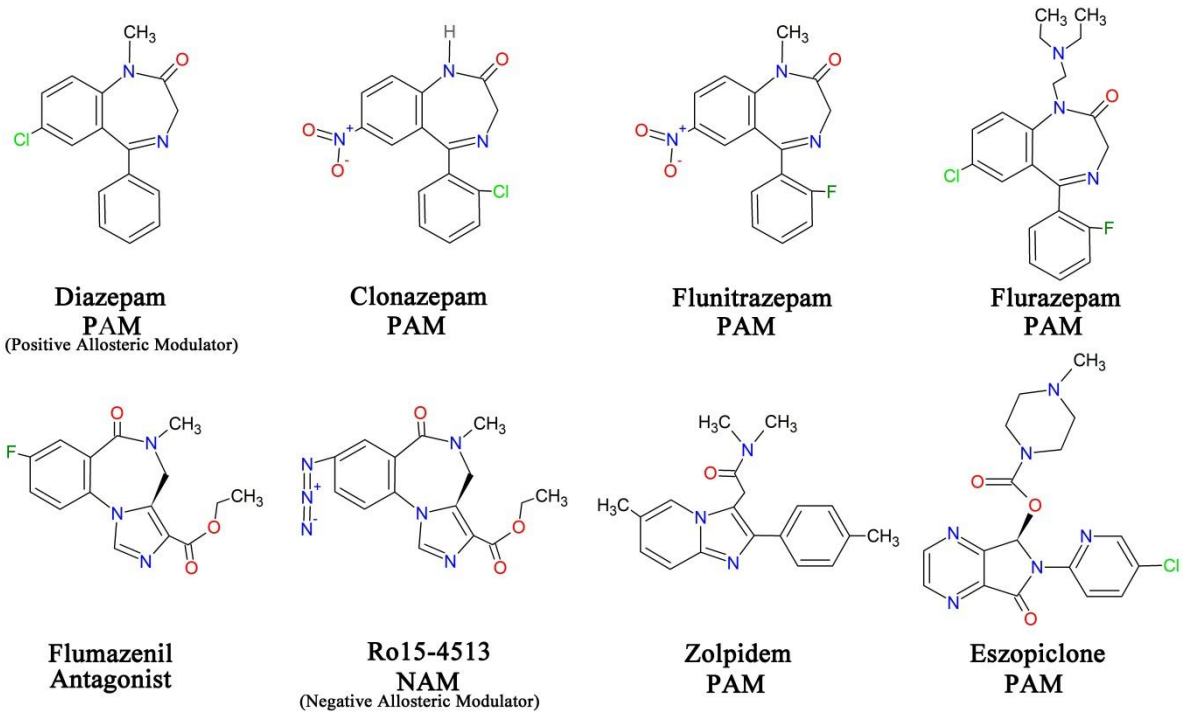

Figure 3. 2D chemical structures of the allosteric ligands employed in this work. Diazepam, Clonazepam, Flunitrazepam, Flurazepam, Ro15-4513, Flumazenil, Zolpidem and Eszopiclone bind with high affinity to the allosteric Benzodiazepines site.

Acetylcholine-binding proteins and non-eukaryotic receptors such as ELIC (Erwinia ligand-gated ion channel), GLIC (Gloeobacter ligand-gated ion channel) and invertebrate Glutamate receptors have been extensively used in the past as templates to model mammalian Cys-Loop receptors (Berezhnoy, Gibbs, & Farb, 2009; Bergmann, Kongsbak, Sørensen, Sander, & Balle, 2013; Bertaccini, Yoluk, Lindahl, & Trudell, 2013; Carpenter, Lau, & Lightstone, 2012; Carpenter & Lightstone, 2016; Cromer, Morton, & Parker, 2002; Ernst, Brauchart, Boresch, & Sieghart, 2003; Hénin, Salari, Murlidaran, & Brannigan, 2014; Newell & Czajkowski, 2003; Puthenkalam et al., 2016; Sander et al., 2011; Thompson, Lester, & Lummis, 2010; Xie, Sha, Wang, & Cheng, 2013). However, in 2014 the first 3D structure of a $GABA_A$ receptor was published by Miller and Aricescu (Miller & Aricescu, 2015). The authors captured the spatial disposition of the atoms of a β_3 homopentamer, in a desensitized closed state, through X-Ray diffraction with a 2.97Å resolution. The desensitized state is proposed to be of high affinity for ligands (Zhang, Xue, Liu, Yang, & Wang, 2013). This new structure is not only a priceless improvement for the modelling of these receptors, which in turn will provide new information to shed light on their structure and functionality, but also constitutes a prototype to analyse the binding of pharmacologically relevant compounds (Wang et al., 2017). Over the years, different techniques have been used to characterize the binding cavities, providing information about the location of the sites and the relevant residues involved directly in the interaction or affecting the efficacy of the different ligands. However, the lack of crystallographic structures of the $\alpha_1\beta_2\gamma_2$ heteropentamer hampers the characterization of both

the specific interactions in the cavity, and the mechanism underlying signal transmission and gating.

Here, using state of the art computational biology tools, we modelled the human $\alpha_1\beta_2\gamma_2$ $GABA_A$ receptor. Subsequently, we characterized the interactions with the cognate ligands by performing docking experiments refined with molecular dynamics (MD) simulations. From the best of our knowledge, this is the first model able to widely explain experimental data on the aforementioned binding cavities. Indeed, it provides an extensive coverage of the relationship between experimental information and structural features of the orthosteric and benzodiazepines binding sites.

Methods

Constructing the model

The first step in the comparative modelling protocol consisted in retrieving the sequences of the α_1, β_2 and γ_2 human subunits from Uniprot (Apweiler et al., 2004; Consortium, 2017): entries *P14867*, *P47870* and *P18507,* respectively. For each subunit we searched for homologous sequences with SSearch (Pearson, 1991). The highest scores corresponded to two structures: the human $GABA_A$ Receptor β_3 homopentamer (**PDB ID: 4COF**) (Miller & Aricescu, 2015) and human Glycine Receptor α_3 homopentamer (**PDB ID: 5CFB**) (Huang, Chen, Michelsen, Schneider, & Shaffer, 2015). Although both of them were captured in the closed state, the former was co-crystallised with agonist benzamidine (desensitized state) while the latter was co-crystallised with an antagonist (closed-basal state). The differences between these structures involve the orientation of the M2 helices and the opening of loop C. The first receptor shows the highest percentage of identity with our sequences: approximately 40.8% with α_1, 91.1% with β_2 and 43.2% with γ_2, while the second shows 41.5% with α_1, 45.4% with β_2 and 41.8% with γ_2. We decided to carry out the modelling using the human β_3 $GABA_A$ Receptor as a template to prioritize a better quality of the sequence alignments. The percentages of identity are above the established threshold for confidence in the modelling (Table S3 – SI) (Chothia & Lesk, 1986).

PROMALS (Pei & Grishin, 2007)**,** HHPRED (Söding, Biegert, & Lupas, 2005) and Swiss Model (Arnold, Bordoli, Kopp, & Schwede, 2006; Biasini et al., 2014; Kiefer, Arnold, Künzli, Bordoli, & Schwede, 2009) were used to generate multiple alignments of the subunits with sequences belonging to other family members, and the crystallized homopentamer. The results from the three web-servers were compared to find differences only in loop F of α_1 subunit. Manual adjustments of two gaps in loop F of the α_1 subunits were applied in order to agree with experimental data (as from reference (Bergmann et al., 2013)).Truncation of intracellular loops were applied to the alignments following reference (Miller & Aricescu, 2015). The IC domain was not modelled due to lack of suitable templates. Indeed, this domain has not been established as involved in the binding of ligands in the ECD essentially due to the long distance between these domains. Naturally, it represents a limit in the implementation of the model to observe global conformational changes such as the opening and closing of the channel pore.

500 initial models were generated with Modeller 9.14 (Webb & Sali, 2002) using the "Automodel class", which only includes spatial restraints obtained from the sequence alignment of the target and template, and required a refinement level "refine.slow". The best model was determined from the top 20 models, ranked according to the lowest value of the Modeller objective function and the "Discrete Optimized Protein Energy" (DOPE) method score (Shen & Sali, 2006), as the one showing the largest percentage of residues in the most favoured region of the Ramachandran plot. ProSa z-score (Wiederstein & Sippl, 2007),Q-mean score (Benkert, Tosatto, & Schomburg, 2008) and PROCHECK (Laskowski, MacArthur, Moss, & Thornton, 1993) results were also taken into account in the selection process. These evaluation webservers have been extensively applied in several works concerning homology modelling (Carpenter et al., 2012; Roy & Mukherjee, 2017). Moreover, the top 20 models were carefully visually inspected to detect abnormalities. The chosen model was refined with Coot (Emsley, Lohkamp, Scott, & Cowtan, 2010) to optimize rotamers and side chain interactions, and PROPKA together with PDB2PQR (Dolinsky, Nielsen, McCammon, & Baker, 2004; Olsson, Søndergaard, Rostkowski, & Jensen, 2011; Rostkowski, Olsson, Søndergaard, & Jensen, 2011) webserver were employed to assign protonation states and optimize hydrogen bond networks.

Docking procedures

In order to find the binding modes of the selected ligands, we conducted a series of molecular docking simulations by two methods: *blind* and *data-driven*. We used these different techniques as a validation for the results when experimental information was not exhaustive enough.

The blind docking was performed with AutoDock Vina (ADV) (Trott & Olson, 2010), using a 25 Å x 23 Å x 20 Å grid centred at appropriate coordinates in each binding site. All the residues predicted by experimental data to be involved in the binding were within the grid-box. We prepared the ligands and the protein with AutoDockTools (Morris et al., 2009) by adding missing hydrogens, combining the non-polar hydrogen atoms and computing Gasteiger charges. For each ligand a maximum of 20 binding modes were requested and the calculations were performed with the highest level of exhaustivity. The cut-off for the number of binding modes was a difference in the binding energy of 3 kcal/mol between the best and worst models. Both simulations with rigid and flexible side chains were performed, showing no considerable difference in the results.

On the other hand, we used HADDOCK 2.2 , High Ambiguity Driven protein-protein Docking (Van Zundert et al., 2016), which employs experimental information about the interaction to establish the preferred binding modes. The experimental data, when available, was introduced as ambiguous interaction restraints (AIR constraints). The docking protocol implemented in the software is described elsewhere (Dominguez, Boelens, & Bonvin, 2003). The water refined structures were clustered using pairwise backbone Root Mean Square Deviation (RMSD) at the interface with a cut-off of 2Å, and analysed according to their average interaction energies (the sum of electrostatic, van der Waals and ambiguous restraints energies) and their average buried surface area. As stated in HADDOCK webserver, the parameterization of the ligands was done with PRODRG (Schüttelkopf & van Aalten, 2004).

We performed molecular docking simulations with four orthosteric ligands: two agonists (GABA and muscimol) and two antagonists (bicuculline and gabazine). The latter were studied although the receptor was modelled in an 'agonist-bound' state with the aim of assessing whether the model is yet adequate for the study of other classes of ligands. Following the same premise, we applied this technique to agonists, antagonists and inverse agonists of the benzodiazepines binding site; all of which are considerably larger than GABA or benzamidine.

The experimental information (Tables 4 and 5 -SI) used for the data-driven docking of each ligand was variable and strongly dependent on the availability. It should be stressed that, as implemented in HADDOCK, only a random 50% of these restraints were actually employed in the docking simulations. For residues of the orthosteric cavity we used the condition that they should interact with α_1Arg67, β_2Tyr97, β_2Glu155, β_2Ser156, β_2Tyr157, β_2Tyr205 and β_2Arg207. However, no particular orientation was introduced as a restraint. As for the benzodiazepines binding cavity, the docking of Diazepam had very specific interactions incorporated as ambiguous restraints, specifically: the chlorine atom of Diazepam with α_1His102 (Duncalfe, Carpenter, Smillie, Martin, & Dunn, 1996; Tan, Baur, Charon, Goeldner, & Sigel, 2009), and C3 of Diazepam with α_1Thr207 and α_1Ser206 of loop C (Tan et al., 2009). For the remaining ligands of the high affinity benzodiazepine's cavity only, the interacting residues were introduced as AIR constraints (Table 1).

Table 1. List of the residues employed as AIR constraints in the guided docking performed with Haddock.

Ligand	Active residues
Clonazepam	α_1His102,α_1Tyr160,α1Ser206,α_1Tyr210,γ_2Tyr58,γ_2Ala79
Flunitrazepam	α_1Phe100,α_1His102,α_1Tyr160,α1Ser206,α_1Tyr210,γ_2Phe77
Flurazepam	α_1Phe100,α_1Tyr210,γ_2Ala79
Ro15-4513	α_1His102, ,α_1Tyr210,γ_2Thr81
Flumazenil	α_1His102, α_1Asn103,α_1Ser159,α_1Tyr160,α_1Gly208,α_1Tyr210,γ_2Ala79
Zolpidem	α_1Phe100,α_1His102,α_1Gly158,α_1Tyr210,γ_2Phe77,γ_2Met130
Eszopiclone	α_1His102,α_1Thr207,α_1Tyr210,γ_2Phe77

The docking poses with the best scores according to both software programs were then analysed to compare the modelled interactions between ligand and receptor with those extracted from literature. The estimation of the energy of binding provided by the software programs was not contrasted with the experimental values due to a lack of direct correlation (refer to Table S8 - SI for a discussion on this subject). Contacting atoms were defined as those separated by a distance shorter than the sum of their van der Waals radii plus 2.75 Å (approximate diameter of a water molecule). Afterwards, we identified through visual

inspection those atoms that were engaged in biologically relevant interactions (i.e. through H-bonds, salt-bridges, hydrophobic or cation-π interactions, among others). These interactions were tabulated and compared with those predicted by experimental studies, and from this comparison we computed two indices: *Precision* and *Recall*. These are statistical quantities that have been used in other works (Davis & Goadrich, 2006; Fierro, Suku, Alfonso-prieto, & Giorgetti, 2017; Goutte & Gaussier, 2005; Raghavan, Bollmann, & Jung, 1989; Saito & Rehmsmeier, 2015) to assess the quality of the binding modes resulting from docking experiments and to evaluate the performance of the techniques. They are respectively defined as:

Precision$= TP/TP + FP$ (1)

Recall$= TP/TP + FN$ (2)

where TP 'True Positives' are residues predicted experimentally as relevant for the binding and found in our models to interact with the ligand; FN 'False Negatives' are the amino acids proposed by the literature to participate in the binding but are not interacting in our models; and FP 'False positives' are residues identified in our models as interacting with the ligands, although experimental data states otherwise, or are those amino acids within a contacting distance from the ligand but are not engaged in biological relevant interactions (Figure S1-SI).

The similarity of ligands might also shed light on their possible orientation inside the binding cavity, since it has been proposed that a relationship exists between structural similarity and a common binding mode (Boström, Hogner, & Schmitt, 2006). We employed OpenBabelGUI, version 2.4.1 (Boyle et al., 2011; Morley, 2016) to calculate Tanimoto's coefficients to quantify the compounds' similarity (Figure S4-SI).

Molecular dynamics simulations

Given the static nature of the docking protocols, the performance of molecular dynamics simulations would allow the ligands and receptor to adapt to the new conformation of the complex. It has been recently shown that in models of protein-ligand interactions of GPCRs, based on comparative modelling with low sequence identity, molecular dynamics simulations allowed for a better representation of the experimental binding configurations (Fierro et al., 2017; Gelis, Wolf, Hatt, Neuhaus, & Gerwert, 2012; Lai, Singer, & Crasto, 2005). We sequentially simulated the modelled receptor with different docked ligands: one molecule of GABA, muscimol, diazepam, clonazepam, flunitrazepam, flurazepam, Ro15-4513, flumazenil, eszopiclone and zolpidem.

The MD simulations were executed with GROMACS (Berendsen, van der Spoel, & van Drunen, 1995; Páll, Abraham, Kutzner, Hess, & Lindahl, 2015) using the SPC water model (Berendsen, Postma, van Gunsteren, & Hermans, 1981) and the GROMOS53A6 force field (Oostenbrink, Villa, Mark, & Van Gunsteren, 2004) for the protein. In all the simulations, the receptor, with the ligand attached, was embedded in a pre-equilibrated 1-palmitoyl-2-oleoyl-phophatidylcholine (POPC) membrane and surrounded by a solution of water and CL-, NA+ ions in a concentration of 0.15 Mol. The Berger (Berger, Edholm, & Jähnig, 1997) parameters

were used to characterize the lipids, and the parameters for the ligands were obtained from the Automated Topology Builder repository (Malde et al., 2011). The protocol consisted of an energy minimization of the system to a potential energy of 500 kJ/mol with Steepest Descent algorithm, secondly a thermalization in the NPT ensemble with the atom P8 of the phospholipids constrained to move on the plane of the membrane using the simulated annealing algorithm, then a protein/ligand-position restrained simulation to relax the interactions with the solvent, and finally the production runs. Van der Waals interactions were limited with a 1.2 nm cut-off and PME algorithm (Darden et al., 1993) was implemented for the electrostatic calculations also with 1.2 nm as cut-off. Verlet algorithm (Páll & Hess, 2013) was employed for neighbour search, and LINCS constraint algorithm (Hess, Bekker, Berendsen, & Fraaije, 1997) was used to restrain bonds' length. The temperature was kept at 310K with Nose-Hoover thermostat (Hoover, 1985; Nosé, 1984) using a coupling constant of t_T=0.8ps, and the pressure at 1bar with Parrinello-Rahman barostat (Parrinello & Rahman, 1981) and using a coupling constant of t_T =10ps and compressibility 4.5 10^5bar. All the simulations consisted in production runs of 100 ns.

Results and discussion

Model construction

The refined sequence alignment of each human subunit with β_3-subunit, which was employed for the modelling process, is depicted in Figure 4. The extracellular and transmembrane domains consisted in 333 residues for α_1 and 332 for β_2 and γ_2.

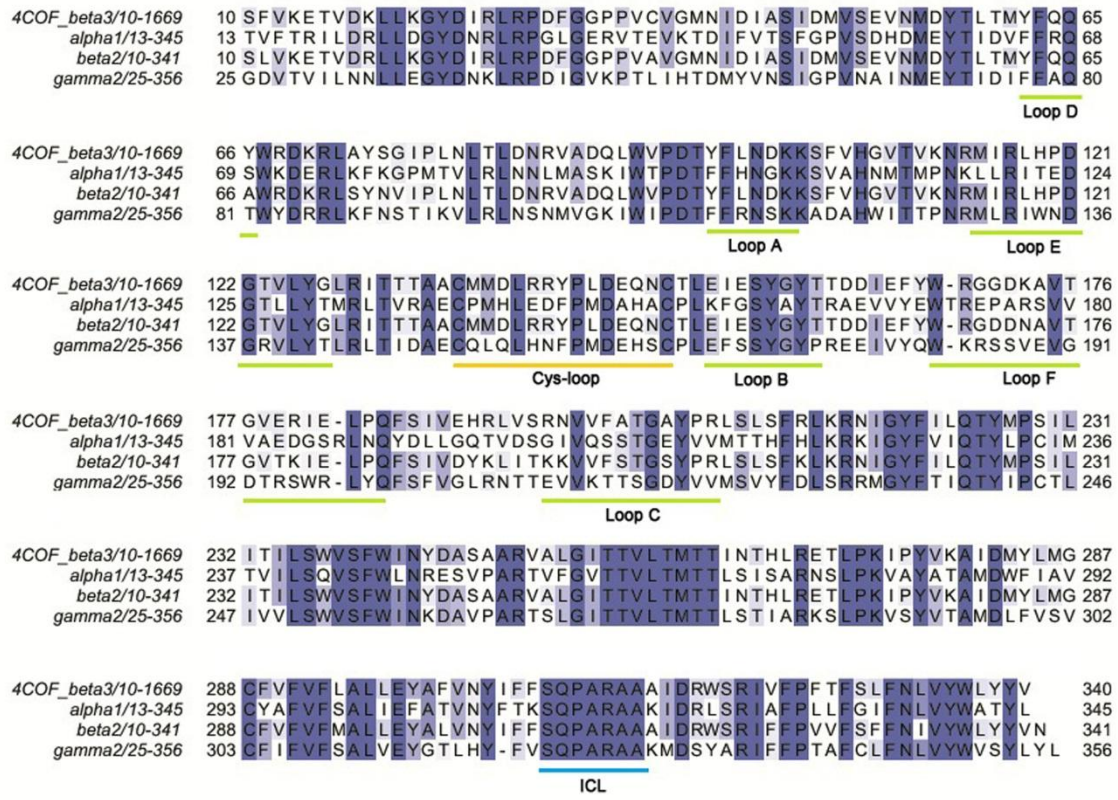

Figure 4. Alignment of the human β_3 subunit (4COF) with human subunits α_1, β_2 and γ_2. The sequences numbering corresponds to the proteins in the mature form. The residues are coloured according to the percentage of identity with the consensus sequence. Dark blue represents an identity of 80% or more, blue corresponds to more than 60%, while light blue represents more than 40% identity. The loops that form the binding cavities are underlined in green, while the emblematic Cys-loop is underlined in yellow. The intracellular linker is underlined in light blue (ICL).

The final model was chosen among the 500 initial configurations by considering structural parameters. The results of Q-mean program (Benkert et al., 2008) showed that the model is slightly improved, compared to a previous model (Bergmann et al., 2013), and acceptable relative to the crystallographic structure (Table S1 – SI). In addition, PROCHECK scores were satisfactory (Table S2- SI) and the Ramachandran plot (Figure 5) confirms the good quality of the backbone geometry, with 99.8% of the residues in the allowed regions.

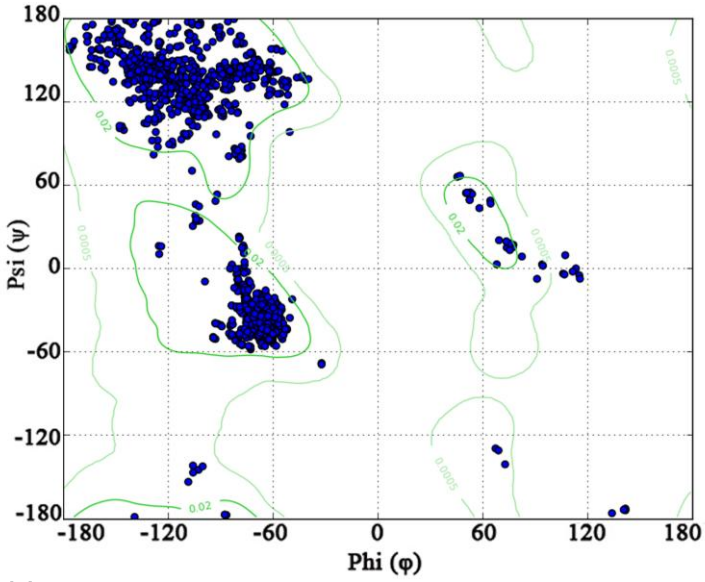

Figure 5. Ramachandran plot of the modelled receptor. 94.2% of the residues are in the most favoured regions, 5.6% in additional allowed regions and 0.2% in generously allowed regions. There are not residues in the disallowed region.

Molecular Docking

We performed *blind* and *data-driven* molecular docking for ligands of the orthosteric and high affinity benzodiazepines' binding cavity. The results were then statistically compared against experimental data available by calculating the recall and precision coefficients. The models that better agreed with experimental data were then funnelled through our analysis protocol.

Orthosteric binding cavity

We carried out docking simulations of four orthosteric ligands in both sites G^1 and G^2 (Figure 1.b and S3). The results presented here belong to site G^1 (except for the docking of bicuculline, which belongs to site G^2), since the observed binding modes were similar in both cavities. In general, all the studies showed very high precision and recall values (Table 2), indicating that there are few residues in the binding cavity that cannot be recognized by the docking protocols or are not available for interaction in our model. One exception is the binding of bicuculline, which shows a better recall value but lower precision. This might be caused by the size of this ligand, which occupies a large fraction of the binding cavity in disregard of the suggested interactions.

Table 2. Precision and recall scores for the performed docking simulations.

Ligand	GABA		Muscimol		Bicuculline		Gabazine	
Docking software	ADV	HADDOCK	ADV	HADDOCK	ADV	HADDOCK	ADV	HADDOCK
Precision	1.00	1.00	0.85	1.00	0.73	_	0.93	1.00
Recall	0.81	0.81	0.79	0.75	0.85	_	0.72	0.76

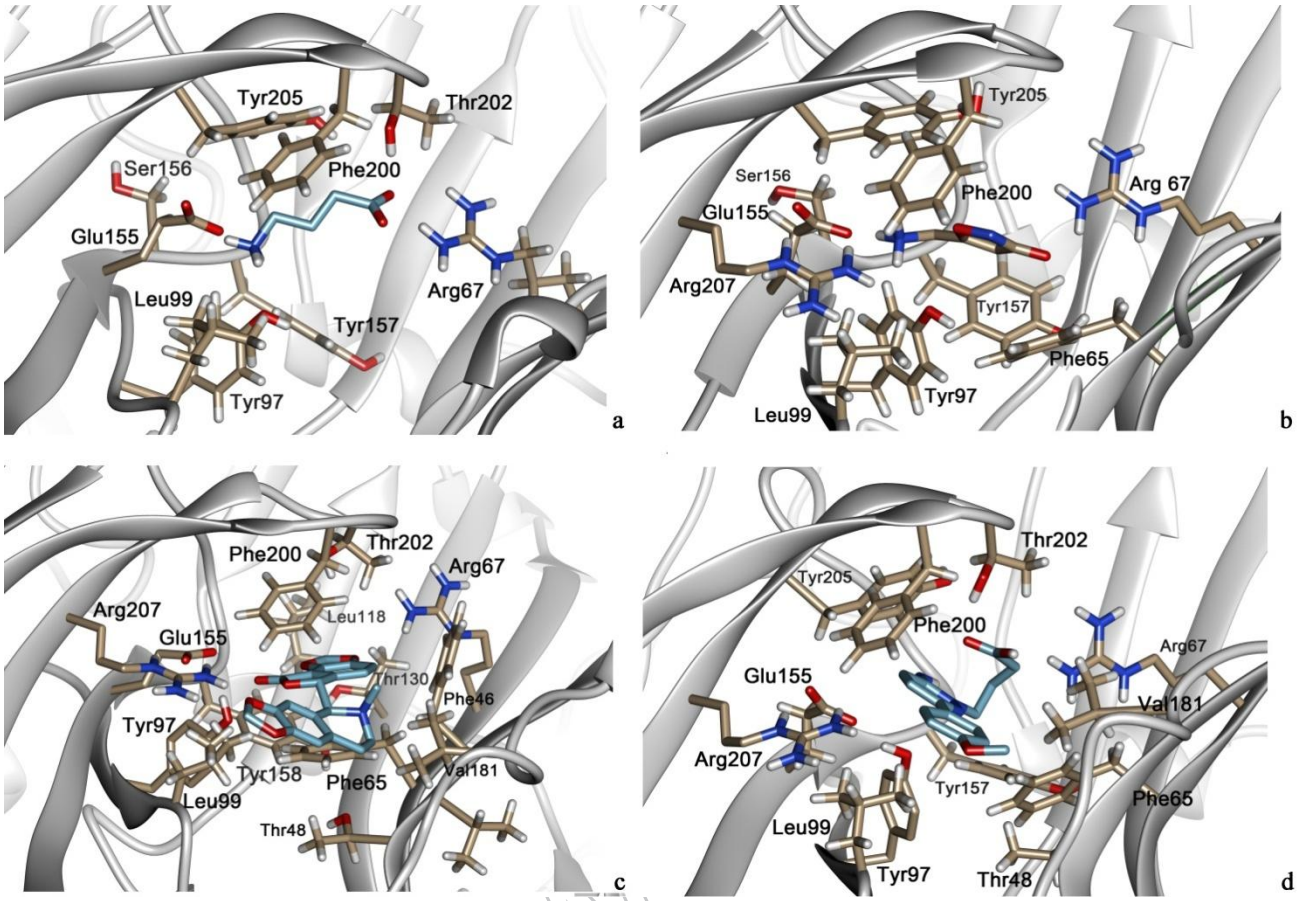

Figure 6. Best docking poses of the ligands of the orthosteric cavity. The configurations displayed correspond to the results with better recall and precision indexes. a. GABA; b. Muscimol; c. Bicuculline; d. Gabazine.

In the best docking mode obtained for GABA (Figure 6.a), the ligand interacts through the amine-end with β_2Glu155 and through the carboxylic group with α_1Arg67, showing complete agreement with experimental information. Likewise, the result of the docking of muscimol (Figure 6.b) shows hydrogen bonds between the protonated amine with β_2Glu155 and the backbone of β_2Ser156 from loop B, and α_1Arg67 with the ketone moiety. This mode agrees partially with previous models (Bergmann et al., 2013)(Sander et al., 2011). We hypothesize that the difficulty in docking bicuculline might be due to the fact that this ligand is an antagonist, and therefore it is expected to bind to the cavity with loop C in a more open conformation, in contrast to our model, which represents an agonist-bound state of the receptor. In our best configuration (Figure 6.c), α_1Phe65 lies parallel to the benzene ring of bicuculline in a plane 3.6 Å below; they are possibly interacting via π-π stacking, in agreement with experimental data. Being smaller than bicuculline, gabazine is able to fit better inside the binding cavity (Figure 6.d). Although the ligand interacts with α_1Arg67 and β_2Arg207 as expected, the experimentally suggested interaction with α_1Asp63 is not present in our docking poses. Interestingly, bicuculline and gabazine displayed contacts with residues from the β-1 strand, namely α_1Phe46, α_1Val47 and α_1Thr48, which, to our knowledge, have not been

explored in experimental studies.

A complete list of the residues involved in interactions with the ligands of the orthosteric cavity in the best binding modes obtained through molecular docking is provided in Table 3.

Table 3. List of residues that participate in the interaction with different ligands of the orthosteric cavity of $GABA_A$Rs.

GABA	Muscimol	Bicuculline	Gabazine
β_2Tyr97	β_2Tyr97	β_2Tyr97	β_2Tyr97
β_2Leu99	β_2Leu99	β_2Leu99	β_2Leu99
β_2Glu155	β_2Glu155	β_2Glu153*	β_2Ser156
β_2Ser156	β_2Ser156	β_2Glu155	β_2Tyr157
β_2Tyr157	β_2Tyr157	β_2Tyr157	β_2Phe200
β_2Gly158	β_2Gly158	β_2Val199*	β_2Thr202
β_2Phe200	β_2Phe200	β_2Phe200	β_2Tyr205
β_2Thr202	β_2Tyr205	β_2Thr202	β_2Arg207
β_2Tyr205	α_1Phe65	β_2Tyr205	α_1Phe46
α_1Phe65	α_1Arg67	β_2Arg207	α_1Thr48
α_1Arg67	α_1Leu118	α_1Phe65	α_1Phe65
α_1Leu118		α_1Arg67	α_1Arg67
		α_1Leu118	α_1Leu118
		α_1Arg120*	α_1Thr130
		α_1Thr130	α_1Val181
		α_1Val180*	
		α_1Val181	

Residues marked with an * are considered false positives.

The docking poses required further refinement since the model considered so far was only a static description of the receptor in a particular state. With this aim, we performed molecular dynamics simulations of the receptor in complex with GABA, as this is the most characterized agonist (Table 4 - SI), and also with muscimol. During the MD simulation, GABA relaxed in the binding cavity and formed i) a cation-π interaction with an aromatic residue, i.e.

β_2Phe200, ii) H-bonds with the tip of loop C, while maintaining the salt-bridges with β_2Glu155 and α_1Arg67 (Figure S9–SI). The network of interactions with this compound was refined in such a way that precision remained in its maximum value, but the recall value improved (Table S6-SI). In addition, it can be appreciated that loop C opened slightly and loop F approached the principal subunit through residue α_1Asp184, which came close to β_2Arg207 (Figure S19– SI). In particular, residue α_1Asp184 has drawn our attention, since it has been proposed as important in GABA binding, although, as it is located in loop F, it is far from the core of the binding site. However, this residue appeared in the docking results of Gabazine, the competitive antagonist, and it is observed that, while GABA remains bound, α_1Asp184 moved towards the principal face of the cavity in molecular dynamics simulations.

β_2Glu153 and β_2Lys196 form a putative salt-bridge that regulates the movements of loop C during activation (Venkatachalan & Czajkowski, 2008). This interaction is supposed to be disrupted upon agonists binding and the consequent conformational change of loop C. In our initial model and throughout the MD simulation, although spatially close (~7 Å), these residues could not form a salt-bridge, which is consistent with the ligand-bound state of the template structure (Venkatachalan & Czajkowski, 2008). Moreover, in the cavity where GABA is bound, β_2Glu153 is part of a stable interacting network which includes β_2Glu155 and β_2Arg207. On the other site, the MD simulation showed a change in the interactions, in which β_2Glu155 now interacts with α_1Arg120 and β_2Arg207 (Figures S20 and S21 –SI). This change in the interaction pattern might be related to the transmission of the agonist signalling.

The MD simulation of muscimol improved both scores to their maximum value (Table S6-SI). The ligand remained in the cavity exploring alternate conformations with orientations that differed in rotations around the main axis of the molecule, engaging in several H-bonds with β_2Ser156, β_2Tyr97, α_1Thr130, β_2Thr202 and α_1Arg120 (Figure S10–SI). The compound spent most of the simulation in a conformation similar to the starting pose.

Benzodiazepines binding cavity

Classical benzodiazepines share, among them, high similarity in their physico-chemical properties. These positive allosteric modulators are expected to bind near residues γ_2Ala79 and α_1His102, in particular the pharmacophore model derived from *in vitro* experiments (Clayton et al., 2007), suggested that the 7-substitutent of classical benzodiazepines should be located between residues Val203, Val212 and Tyr210 from loop C and His102 of loop A (Duncalfe et al., 1996) (Figure S5 – SI).

Table 4. Recall and precision indices of the docking results of ligands of the high affinity benzodiazepines binding cavity on the $GABA_A$ receptor.

Ligand	Diazepam		Clonazepam		Flunitrazepam		Flurazepam		Ro15-4513		Flumazenil		Zolpidem		Eszopiclone	
Software	ADV	Haddock	ADV	Haddock	ADV	Haddock	ADV	Haddock	ADV	Haddock	ADV	Haddock	ADV	Haddock	ADV	Haddock

Precision	0.81	0.81	0.92	0.71	0.92	0.78	0.75	0.87	0.88	0.88	0.88	0.93	0.87	0.88	0.93	0.50
Recall	0.76	0.81	0.65	0.59	0.80	0.43	0.75	0.81	0.94	0.94	0.83	0.83	0.93	0.94	0.93	0.77

The best result for the docking of diazepam (Figure 7.a) displays its chlorine atom pointing towards α_1His102, α_1Asn103 and γ_2Asn60 and the C3 atom in the vicinity of the tip of loop C. In addition, the phenyl ring is surrounded by a hydrophobic cavity formed by α_1Phe100, γ_2Phe77, α_1Tyr160 and α_1Tyr210. As proposed in literature, the N-methyl substituent points outside the binding cavity (Tan et al., 2009) and the benzodiazepine ring lies above γ_2Tyr58 in a parallel plane. Both precision and recall indices are high. Moreover, this configuration agrees well with those proposed by previous works (Berezhnoy et al., 2009; Middendorp et al., 2014) and with experimental information (Clayton et al., 2007, Table 5 -SI). We compared this docking pose with those reported by Richter et al. (2012), finding our model resembles their second ranked mode, since it places the pending phenyl ring inside the lipophilic cavity in the back of the binding site, in contrast to their best binding pose which orients the ring outwards. The rest of the classic benzodiazepines also display high values of both precision and recall (Table 4). For these ligands, except Flunitrazepam (Figure 7.c), the pending phenyl ring is surrounded by the characteristic hydrophobic cavity. Flunitrazepam's 7-substituent (a fluorine atom) interacts with α_1His102 and γ_2Tyr58, which cannot be completely fulfilled by flurazepam (Figure 7.d), whose chlorine atom only interacts with γ_2Tyr58 or by clonazepam (Figure 7.b), which locates the nitro group above γ_2Tyr58 and ~7Å from α_1His102. Remarkably, most of the interactions in the cavity are hydrophobic, which might account for the high values of the indices. Most of the residues involved in the binding of these ligands (Table 5) are the same as the ones suggested in the literature (Table S5 - SI).

Bearing in mind the information available regarding the binding of diazepam, we performed two MD simulations, starting with the best configurations obtained from both docking methods. Throughout the simulations, Diazepam changed its orientation to adopt an almost identical configuration in the binding cavity for both MD simulations; the precision and recall scores exhibited small differences due to alternative disposition of the surrounding side chains. However, the final refined model showed improved indices (Tables S6 and S7 - SI). On the other hand, along the MD simulations of clonazepam, this ligand sampled different conformations within the cavity so that the benzodiazepine ring lays parallel to the membrane plane, the nitro group points outside the cavity and the chloro-phenyl ring remains in the hydrophobic cavity. During the simulation with flunitrazepam the side-chains of surrounding residues relaxed in the cavity, while the ligand remained virtually motionless, improving slightly both evaluation parameters. The second best docking pose obtained for flurazepam (Figure 7.d), although it shows lower precision and recall scores, resembles the pose adopted by bromoflurazepam while interacting with the prokaryotic receptor ELIC (Spurny et al., 2012) in one of its crystallographic structures (PDB ID: 4A98). Thus, we used this configuration to perform the MD simulations. Along the simulations, the ligand undergoes several changes in its orientation to finally converge to a conformation resembling the starting pose.

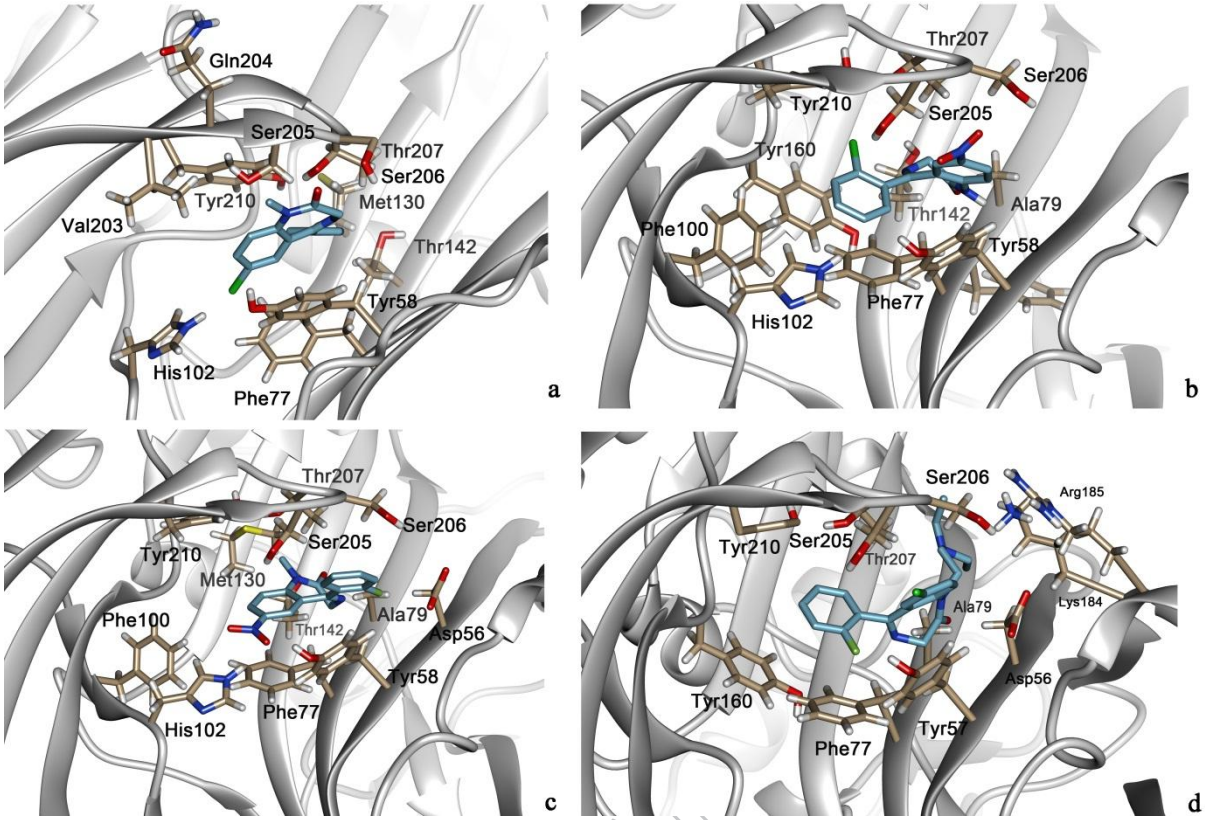

Figure 7. Best docking modes of the classic BZDs. a. Diazepam, b. Clonazepam, c. Flunitrazepam, d. Flurazepam.

Regarding the imidazo-benzodiazepines (i-BZD), while they show high similarity between them, they are very different compared to classical benzodiazepines (Figure S4 –SI). Mutation and SCAM studies have shown that the 3' substituent of the i-BZD's imidazo-ring is located nearby γ_2Ala79 and γ_2Thr81 (Kucken, Teissére, Seffinga-clark, Wagner, & Czajkowski, 2003), and the 7-substituent should be pointing towards α_1His102, α_1Val203, α_1Val212 and α_1Gly158 from loop B (Tan et al., 2007). α_1Tyr210 is proposed to photoincorporate Ro15-4513, with the azide group pointing towards that region (Sawyer, Chiara, Olsen, & Cohen, 2002). The best docking configurations of Ro15-4513 (Figure 8.a) and flumazenil (Figure 8.b) have their imidazo 3'-substituent pointing towards γ_2Ala79 and the 7-substituent pointing towards α_1His102. Additionally, α_1Tyr210 interacts directly with Ro15-4513. Both models are in agreement with the requirements of the pharmarcophore model (Clayton et al., 2007). However, there are discrepancies regarding the orientation of the 4th and 5th positions of the benzodiazepine ring: these atoms point into the interior of the binding cavity in some of our models, but in one of the bests configurations obtained for Ro15-4513 the imidazole ring is orientated inwards, while these atoms point outwards. Previous models have oriented these atoms to the exterior of the cavity (Kucken et al., 2003) similar to the behaviour of the N-methyl and carbonyl moieties in Diazepam.

Since the binding modes for Ro15-4513 show identical scores (Table 4), we performed

MD simulations for both systems. The model with the imidazole ring pointing inwards displayed better results: The simulation improved the precision and recall scores (Table 6), and the ligand adopted a stable configuration with loop C in an open conformation. Regarding the binding mode of flumazenil, MD simulations were not able to improve the docking precision and recall values. In our docking studies the best binding modes differed in the orientation of the imidazole ring. Considering that the MD simulations of Ro15-4513 gave better results for the system with the ligand oriented so that the imidazole ring points into the cavity, we believe that binding mode of flumazenil should also reproduce this feature.

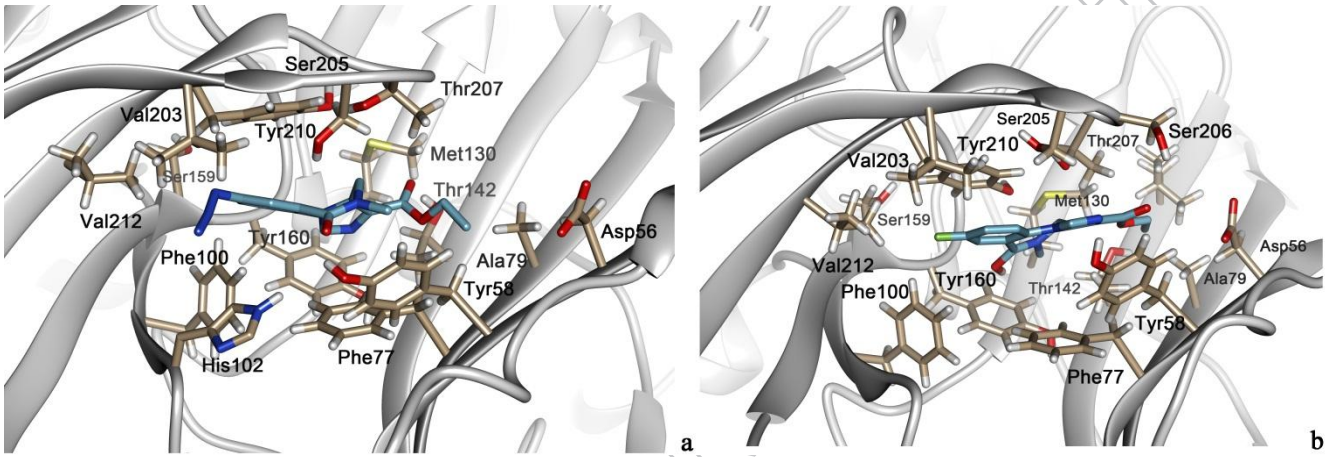

Figure 8. Best docking modes of the i-BZDs according to precision and recall scores. a. Ro15-4513, b. Flumazenil.

The docking studies of zolpidem resulted in very similar conformations which displayed comparable recall and precision indexes (Table 4). The observed interactions are mostly hydrophobic (Table 5). It has been already proposed that, since it does not share many polar interactions, the binding mode of zolpidem depends more on the shape of the cavity rather than on the interaction with particular residues (Hanson, Morlock, Satyshur, & Czajkowski, 2008). The best configuration (Figure 9.a) can be related to previous computational studies performed with a different model (Vijayan, Bhattacharyya, & Ghoshal, 2012) and with the pharmacophore model based on experimental information (Clayton et al., 2007). However, in our model there is no direct interaction between the ligand and loop F as proposed in literature (Table 5 – SI).

Concerning the docking of eszopiclone (Figure 9.b), the best binding mode possesses high indices of precision and recall (Table 4) and agrees well with the pharmacophore model based on experimental data (Clayton et al., 2007). In addition, the orientation is similar to the one adopted by R-zopiclone bound to ELIC receptor (Spurny et al., 2012) (PDB ID: 4A97). Both ligands share common interactions with conserved aromatic residues (Table 5), even though the spatial disposition of the side-chains is not exactly preserved. The chlorine atom is oriented towards the back of the cavity, between α_1Tyr160 and α_1Tyr210 and the methyl-piperazine group is located near α_1His102 and α_1Phe100, while the pyridine ring interacts with γ_2Phe77

and α_1Thr206. The pyrrolo-pyrazin is located under the tip of loop C and above γ_2Tyr58. The free carboxyl interacts with γ_2Tyr58 through and H-bond. A docking mode similar to that proposed by Hanson et al. (Hanson et al., 2008) was also found with ADV with the same binding score.

Both ligands remained bound during the MD simulations, with eszopiclone temporarily exploring other conformations along its simulation while zolpidem retained its orientation. Even though precision was increased for both ligands, recall was somewhat reduced (Table 6).

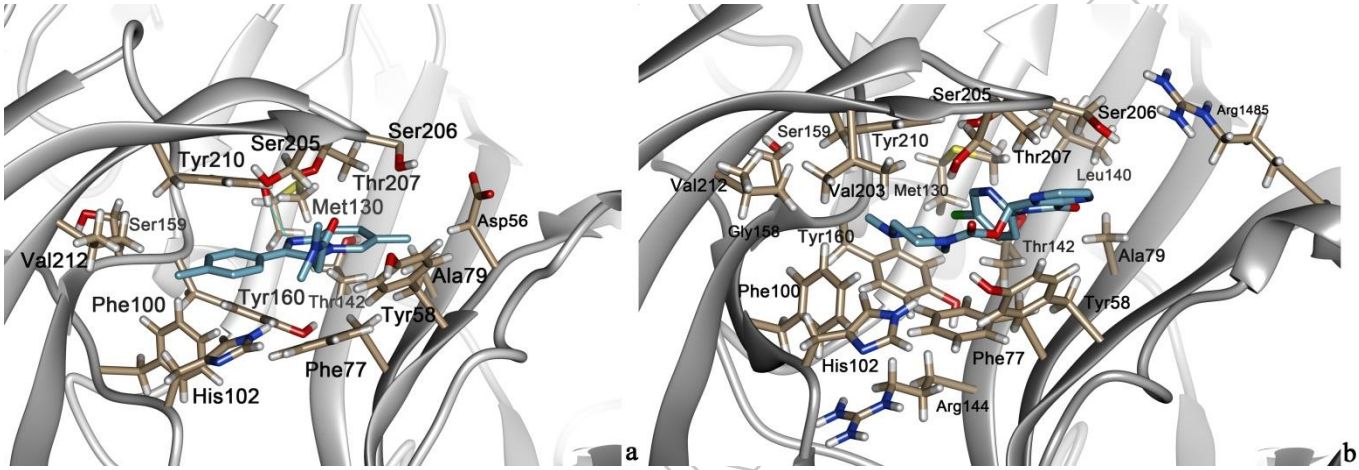

Figure 9. Best docking modes of two of the non-benzodiazepine compounds that bind to the high affinity benzodiazepine binding site. a. Zolpidem, b. Eszopiclone.

Table 5. List of residues that participate on the interaction with ligands of the high affinity benzodiazepines binding cavity of our modelled $GABA_AR$.

Diazepam	Clonazepam	Flunitrazepam	Flurazepam	Ro154513	Flumazenil	Zolpidem	Eszopiclone
α_1His102	α_1Phe100	α_1Phe100	α_1Phe100	α_1Phe100	α_1Phe100	α_1Phe100	α_1Phe100

α_1Tyr160	α_1His102	α_1His102	α_1His102	α_1His102	α_1His102	α_1His102	α_1His102
α_1Val203	α_1Tyr160	α_1Tyr160	α_1Lys156*	α_1Gly158	α_1Tyr160	α_1Gly158	α_1Gly158
α_1Ser205	α_1Ser205*	α_1Ser205	α_1 Ser159	α_1Ser159	α_1Val203	α_1Ser159	α_1Ser159
α_1Ser206	α_1Ser206	α_1Ser206	α_1Tyr160	α_1Tyr160	α_1Ser205	α_1Tyr160	α_1Tyr160
α_1Thr207	α_1Thr207	α_1Thr207	α_1Val203	α_1Val203	α_1Ser206	α_1Val203	α_1Val203
α_1Tyr210	α_1Tyr210	α_1Tyr210	α_1Gln204*	α_1Ser205	α_1Thr207	α_1Ser205	α_1Ser205
γ_2Asp56*	γ_2Asp56	γ_2Asp56*	α_1Ser205*	α_1Ser206	α_1Tyr210	α_1Ser206*	α_1Ser206*
γ_2Tyr58	γ_2 Tyr 58	γ_2Tyr58	α_1Ser206	α_1Thr207	α_1Val212	α_1Thr207	α_1Thr207
γ_2Asn60*	γ_2Phe77	γ_2Phe77	α_1Thr207	α_1Tyr210	γ_2Asp56*	α_1Tyr210	α_1Tyr210
γ_2Phe77	γ_2 Ala 79	γ_2Ala79	α_1Tyr210	α_1Val212	γ_2Tyr58	α_1 Val212	α_1Val212
γ_2Ala79	γ_2Met130	γ_2Met130	α_1Val212	γ_2Asp56*	γ_2Phe77	γ_2Asp56*	γ_2Tyr58
γ_2Met130	γ_2Leu140	γ_2Thr142	γ_2Tyr58	γ_2Tyr58	γ_2Ala79	γ_2Tyr58	γ_2Phe77
γ_2Thr142	γ_2Thr142		γ_2Phe77	γ_2Phe77	γ_2Met130	γ_2Phe77	γ_2Ala 79
γ_2Gly191			γ_2Met130	γ_2Ala79	γ_2Leu140	γ_2Ala79	γ_2Met130
γ_2Arg192*			γ_2Thr142	γ_2Met130*	γ_2Thr142	γ_2Met130	γ_2Thr142
				γ_2Thr142		γ_2Leu140	
						γ_2Thr142	

Residues marked with an * were considered false positives.

There are certain residues suggested in literature (Table 5 -SI) as relevant in the

binding of ligands but which are not observed in any of our models to have an active interaction with the compounds. For instance, residue α_1Gly201 is located at the base of loop C; its mutation probably affects the binding of the ligands (zolpidem and eszopiclone) because longer chains might alter the movement capacity of this loop. This mutation might also modify the orientation of the neighbouring side-chains and directly affect the entrance of the ligand (Hanson et al., 2008). Regarding the hypothetical interaction of flunitrazepam and zolpidem with γ_2Met57, from our models we suggest that it may be very difficult for the side chain of this residue to interact directly with the ligands, because it is located in a beta strand with the side chain oriented outwards in the cavity. In addition, considering the following residue is γ_2Tyr58, which has also been proved to directly interact with ligand, the disposition of the amino acids in the secondary structure seems correct. On the other hand, the experimentally observed reduction of binding affinities when α_1Gly158 or α_1Gly208 are mutated to Cys (Table 5 – SI), can be explained by our model since a mutation in these positions would severely reduce the available volume of the cavity and alter the interactions between residues. The mutation α_1G158C makes it possible for Ro15-4513 to interact with this residue through its azide moiety, as suggested experimentally (Tan et al., 2007).

Essentially, the refinement MD simulations performed on the receptor in complex with the allosteric modulators, improved both recall and precision indices (Tables S6 and S7 - SI). All of the ligands remained bound to the cavity within the 100ns of simulation and most of them did not change their orientation drastically (Figures S11-S18 –SI). Flurazepam and diazepam displayed the most noticeable movements. The stability of the complexes and the ligands within the binding cavity was ascertained through measurements of the root-mean-square deviation (RMSD) (Figures S7 and S8 – SI).

Table 6. Recall and precision for chosen ligands before and after MD Simulations.

Ligand	Diazepam		Clonazepam		Flunitrazepam		Flurazepam		Ro15-4513		Flumazenil		Zolpidem		Eszopiclone	
Software	ADV	MD	ADV	MD	ADV	MD	ADV	MD	ADV	MD	Haddock	MD	Haddock	MD	ADV	MD
Precisio	0.8	1.0	0.92	0.88	0.92	0.93	0.87	0.94	0.8	0.9	0.93	0.7	0.88	1.0	0.93	1

n	1	0							8	4		9		0				
Recall	0.76	0.87	0.65	0.88	0.80	0.93	0.81	0.83	0.94	0.94	0.83	0.73	0.94	0.88	0.93	0.88		

As a final remark, this work could provide a starting point for the design of several experimental studies. On the one hand, confirmation of the binding modes for the ligands is needed. On the other hand, we observed potential interactions between the ligands and unexplored regions of the receptor such as the amino acids from the β-1 strand in the orthosteric binding pocket, thus, we propose that mutational and substituted-cysteine accessibility method (SCAM) analysis would contribute greatly to understand the participation of these residues, which have been proposed to participate in the binding process in analogy with the benzodiazepines' binding site (Kucken et al., 2000). The approach of loop F of the orthosteric cavity towards the principal face through α_1Asp184 in the MD simulations is a hint on the mechanisms involving this loop. Thus we propose cross-linking and mutational studies should be performed on this residue in order to asses its role in the binding and activation of the channel, and the allosteric influence of benzodiazepines.

Conclusions

Due to their role in neurological health and vast pharmacology, the study of the structure of $GABA_A$ receptors, their function and interactions with other molecules is essential to understand the bases of many diseases and develop new treatments, as well as strategies for improving life quality.

It was not until 2014 that the first crystallographic structure of a $GABA_A$ receptor was published. For this reason, previous models were performed with templates sharing very low sequence identity belonging to other receptors of the Cys-loop family and AChBPs. In this work, we present a model of the $\alpha_1\beta_2\gamma_2$ $GABA_A$ receptor in a closed-desensitized state based on the human β_3 homopentamer (Figure S2 – SI). The model here presented is able to reproduce active binding cavities, as they have been validated against all the existing experimental data.

Due to the lack of a heteromeric structure in the apo-state or with bound ligands, state-of-the-art computational studies can be combined with experimental data to obtain information about the binding and conformational changes in the receptor that lead to its opening and closing. Docking results, although sometimes ambiguous, allowed us to propose binding modes for different ligands and helped in the formulation of hypotheses about the important residues. In this work, the docking procedures were able to capture the main features of the interaction of the receptor and its cognate ligands. Refinement using MD simulations allowed us to improve the results by providing a more extensive sampling of the conformational space of the ligand interacting with the receptor.

Regarding the binding properties of ligands of the orthosteric cavity, agonists GABA and muscimol could be docked in conformations that are similar for both compounds, in agreement with previous works (Bergmann et al., 2013; Boileau, Evers, Davis, & Czajkowski,

1999; Goldschen-Ohm, Wagner, & Jones, 2011; Holden & Czajkowski, 2002; Newell, McDevitt, & Czajkowski, 2004; Sander et al., 2011). Bicuculline, however, could not be located in a precise configuration in this model of the receptor, probably due to its size and the fact that it is an antagonist, and therefore it is expected to bind in the cavity with loop C in an open conformation. While gabazine, being smaller, fitted well into the cavity and was engaged in several of the suggested interactions (Boileau et al., 1999; Newell et al., 2004; Padgett, Hanek, Lester, Dougherty, & Lummis, 2007; Wagner & Czajkowski, 2001; Westh-Hansen et al., 1999) (Table 4 of the SI).

The current information about the high affinity benzodiazepines binding cavity allowed us to propose a binding mode for diazepam which is able to explain the available experimental data (Clayton et al., 2007;Hanson & Czajkowski, 2008; Middendorp et al., 2014; Tan et al., 2009, Table S5-SI). Other classical benzodiazepines, namely clonazepam, flunitrazepam and flurazepam, were docked in modes that are compatible with experimental data but which do not share exactly the same binding features as diazepam. The imidazo-benzodiazepines could also be docked based on experimental information (Kucken et al., 2003; Middendorp et al., 2014; Morlock & Czajkowski, 2011), showing that this site, in our model, is capable of binding not only positive modulators, but also antagonists and negative modulators. Non-benzodiazepine drugs zolpidem and eszopiclone exhibited binding modes that are also in agreement with experimental data (Hanson et al., 2008). Remarkably, the docking of eszopiclone could be directly compared to the crystallographic structure of R-zopiclone bound to a prokariotic homologue receptor (ELIC) (Spurny et al., 2012). Both ligands show high similarity in the orientation within the cavity and make common key contacts with homologous hydrophobic residues of the binding sites.

In conclusion, we built a model of the $\alpha_1\beta_2\gamma_2$ $GABA_A$ receptor, comprising both the extracellular and transmembrane domains, which was then docked with compounds of the orthosteric and benzodiazepines binding sites. All the described complexes are in agreement with the available experimental data. We therefore suggest that this model can be used in future studies related to the orthosteric and benzodiazepines binding sites. Additionally, we propose that mutational and SCAM analysis would contribute greatly to understand the participation of amino acids from the β-1 strand in the orthosteric cavity. Finally, we consider that this model might contribute to the future development of novel strategies for the design of specific orthosteric/allosteric ligands.

Acknowledgments

We would like to thank Universidad Nacional del Sur, IFISUR-CONICET and Università degli Studi di Verona.

Funding

This work was supported by Universidad Nacional del Sur (UNS) under Grant [PGI 24/F064]; IFISUR (UNS/CONICET), Bahía Blanca. FZ and MJA are fellows of CONICET.

References

Apweiler, R., Bairoch, A., Wu, C. H., Barker, W. C., Boeckmann, B., Ferro, S., … others. (2004). UniProt: the universal protein knowledgebase. *Nucleic Acids Research*, *32*(suppl_1), D115--D119.

Arnold, K., Bordoli, L., Kopp, J., & Schwede, T. (2006). The SWISS-MODEL workspace: a web-based environment for protein structure homology modelling. *Bioinformatics*, *22*(2), 195–201. http://doi.org/10.1093/bioinformatics/bti770

Benkert, P., Tosatto, S. C. E., & Schomburg, D. (2008). QMEAN: A comprehensive scoring function for model quality assessment. *Proteins: Structure, Function, and Bioinformatics*, *71*(1), 261–277. http://doi.org/10.1002/prot.21715

Berendsen, H. J. C., Postma, J. P. M., van Gunsteren, W. F., & Hermans, J. (1981). Interaction Models for Water in Relation to Protein Hydration. In *Intermolecular Forces* (pp. 331–342). Springer Netherlands. http://doi.org/10.1007/978-94-015-7658-1_21

Berendsen, H. J. C., van der Spoel, D., & van Drunen, R. (1995). GROMACS: A message-passing parallel molecular dynamics implementation. *Computer Physics Communications*, *91*(1–3), 43–56. http://doi.org/10.1016/0010-4655(95)00042-E

Berezhnoy, D., Gibbs, T. T., & Farb, D. H. (2009). Docking of 1 ,4-Benzodiazepines in the alpha1 / gamma2 GABA A Receptor Modulator Site. *Molecular Pharmacology*, *76*(1998), 440–450. http://doi.org/10.1124/mol.109.054650.

Berger, O., Edholm, O., & Jähnig, F. (1997). Molecular dynamics simulations of a fluid bilayer of dipalmitoylphosphatidylcholine at full hydration, constant pressure, and constant temperature. *Biophysical Journal*, *72*(5), 2002–2013.

Bergmann, R., Kongsbak, K., Sørensen, P. L., Sander, T., & Balle, T. (2013). A Unified Model of the GABAA Receptor Comprising Agonist and Benzodiazepine Binding Sites. *PLoS ONE*, *8*(1), 1–13. http://doi.org/10.1371/journal.pone.0052323

Bertaccini, E. J., Yoluk, O., Lindahl, E. R., & Trudell, J. R. (2013). Assessment of homology templates and an anesthetic binding site within the gamma-aminobutyric acid receptor. *Anesthesiology*, *119*(5), 1087–1095. http://doi.org/10.1097/ALN.0b013e31829e47e3

Biasini, M., Bienert, S., Waterhouse, A., Arnold, K., Studer, G., Schmidt, T., … Schwede, T. (2014). SWISS-MODEL: modelling protein tertiary and quaternary structure using

evolutionary information. *Nucleic Acids Research*, *42*(W1), W252–W258. http://doi.org/10.1093/nar/gku340

Boileau, A. J., Evers, A. R., Davis, A. F., & Czajkowski, C. (1999). Mapping the Agonist Binding Site of the GABAAReceptor: Evidence for a β-Strand. *Journal of Neuroscience*, *19*(12), 4847–4854. Retrieved from http://www.jneurosci.org/content/19/12/4847

Boström, J., Hogner, A., & Schmitt, S. (2006). Do Structurally Similar Ligands Bind in a Similar Fashion ? *Journal of Medicinal Chemistry*, *49*(23), 6716–6725. http://doi.org/10.1021/jm060167o

Boyle, N. M. O., Banck, M., James, C. A., Morley, C., Vandermeersch, T., & Hutchison, G. R. (2011). Open Babel : An open chemical toolbox. *Journal of Cheminformatics*, *3*(33), 1–14. http://doi.org/10.1186/1758-2946-3-33

Calimet, N., Simoes, M., Changeux, J.-P., Karplus, M., Taly, A., & Cecchini, M. (2013). A gating mechanism of pentameric ligand-gated ion channels. *Proceedings of the National Academy of Sciences of the United States of America*, *110*(42), E3987-96. http://doi.org/10.1073/pnas.1313785110

Carpenter, T. S., Lau, E. Y., & Lightstone, F. C. (2012). A Role for Loop F in Modulating GABA Binding Affinity in the GABA A Receptor. *Journal of Molecular Biology*, *422*(2), 310–323. http://doi.org/10.1016/j.jmb.2012.05.025

Carpenter, T. S., & Lightstone, F. C. (2016). An Electrostatic Funnel in the GABA-Binding Pathway. *PLoS Computational Biology*, *12*(4), 1–23. http://doi.org/10.1371/journal.pcbi.1004831

Changeux, J. P., & Edelstein, S. J. (1998). Allosteric receptors after 30 years. *Neuron*, *21*(5), 959–980. http://doi.org/https://doi.org/10.1016/S0896-6273(00)80616-9

Chothia, C., & Lesk, A. M. (1986). The relation between the divergence of sequence and structure in proteins. *The EMBO Journal*, *5*(4), 823–826. Retrieved from http://www.pubmedcentral.nih.gov/articlerender.fcgi?artid=1166865&tool=pmcentrez&rendertype=abstract

Clayton, T., Chen, J. L., Ernst, M., Richter, L., Cromer, B. a, Morton, C. J., … Cook, J. M. (2007). An updated unified pharmacophore model of the benzodiazepine binding site on gamma-aminobutyric acid (A) receptors: correlation with comparative models. *Current Medicinal*

Chemistry, *14*(26), 2755–2775. http://doi.org/10.2174/092986707782360097

Collins, A. L., Ma, D., Whitehead, P. L., Martin, E. R., Wright, H. H., Abramson, R. K., … Pericak-Vance, M. A. (2006). Investigation of autism and GABA receptor subunit genes in multiple ethnic groups. *Neurogenetics*, *7*(3), 167–174. http://doi.org/10.1007/s10048-006-0045-1

Consortium, T. U. (2017). UniProt: the universal protein knowledgebase. *Nucleic Acids Research*, *45*(D1), D158--D169. http://doi.org/10.1093/nar/gkw1099

Crestani, F., Lorez, M., Baer, K., Essrich, C., Benke, D., Laurent, J. P., … Mohler, H. (1999). Decreased GABAA-receptor clustering results in enhanced anxiety and a bias for threat cues. *Nature Neuroscience*, *2*(9), 833–839.

Cromer, B. a, Morton, C. J., & Parker, M. W. (2002). Anxiety over GABA A receptor structure relieved by AChBP. *Trends in Biochemical Sciences*, *27*(6), 280–287.

Darden, T., York, D., Pedersen, L., Darden, T., York, D., & Pedersen, L. (1993). Particle mesh Ewald : An Nlog (N) method for Ewald sums in large systems. *The Journal of Chemical Physics*, *98*(12), 10089–10092. http://doi.org/10.1063/1.464397

Davis, J., & Goadrich, M. (2006). The relationship between Precision-Recall and ROC curves. In *Proceedings of the 23rd international conference on Machine learning* (pp. 233–240). ACM. http://doi.org/10.1145/1143844.1143874

Dolinsky, T. J., Nielsen, J. E., McCammon, J. A., & Baker, N. a. (2004). PDB2PQR: an automated pipeline for the setup of Poisson-Boltzmann electrostatics calculations. *Nucleic Acids Research*, *32*(Web Server issue), W665-7. http://doi.org/10.1093/nar/gkh381

Dominguez, C., Boelens, R., & Bonvin, A. M. (2003). HADDOCK: a protein− protein docking approach based on biochemical or biophysical Information. *Journal of the American Chemical Society*, *125*(7), 1731–1737. http://doi.org/10.1021/ja026939x

Duncalfe, L. L., Carpenter, M. R., Smillie, L. B., Martin, I. L., & Dunn, S. M. (1996). The major site of photoaffinity labeling of the gamma-aminobutyric acid type A receptor by [3H]flunitrazepam is histidine 102 of the alpha subunit. *The Journal of Biological Chemistry*, *271*(16), 9209–9214. http://doi.org/10.1074/jbc.271.16.9209

Emsley, P., Lohkamp, B., Scott, W. G., & Cowtan, K. (2010). Features and Development of Coot. *Acta Crystallographica Section D - Biological Crystallography*, *66*(4), 486–501. http://doi.org/10.1107/S0907444910007493

Ernst, M., Brauchart, D., Boresch, S., & Sieghart, W. (2003). Comparative modeling of GABAA receptors: Limits, insights, future developments. *Neuroscience*, *119*(4), 933–943. http://doi.org/10.1016/S0306-4522(03)00288-4

Fierro, F., Suku, E., Alfonso-prieto, M., & Giorgetti, A. (2017). Agonist Binding to Chemosensory Receptors : A Systematic Bioinformatics Analysis. *Frontiers in Molecular Biosciences*, *4*(September), 1–14. http://doi.org/10.3389/fmolb.2017.00063

Gelis, L., Wolf, S., Hatt, H., Neuhaus, E. M., & Gerwert, K. (2012). Prediction of a Ligand-Binding Niche within a Human Olfactory Receptor by Combining Site-Directed Mutagenesis with Dynamic Homology Modeling. *Angewandte Chemie International Edition*, *51*(5), 1274–1278. http://doi.org/10.1002/anie.201103980

Goldschen-Ohm, M., Wagner, D., & Jones, M. (2011). Three arginines in the GABAA receptor binding pocket have distinct roles in the formation and stability of agonist-versus antagonist-bound complexes. *Molecular Pharmacology*, *80*(4), 647–656. http://doi.org/10.1124/mol.111.072033.2002

Goutte, C., & Gaussier, E. (2005). A probabilistic interpretation of precision, recall and F-score, with implication for evaluation. In *ECIR* (Vol. 5, pp. 345–359).

Hanson, S. M., & Czajkowski, C. (2008). Structural mechanisms underlying benzodiazepine modulation of the GABA(A) receptor. *The Journal of Neuroscience*, *28*(13), 3490–9. http://doi.org/10.1523/JNEUROSCI.5727-07.2008

Hanson, S. M., Morlock, E. V., Satyshur, K. A., & Czajkowski, C. (2008). Structural Requirements for Eszopiclone and Zolpidem Binding to the γ-Aminobutyric Acid Type-A (GABAA) Receptor Are Different. *Journal of Medicinal Chemistry*, *51*(22), 7243–7252. http://doi.org/10.1021/jm800889m

Hénin, J., Salari, R., Murlidaran, S., & Brannigan, G. (2014). A predicted binding site for cholesterol on the GABAA receptor. *Biophysical Journal*, *106*(9), 1938–1949. http://doi.org/10.1016/j.bpj.2014.03.024

Hess, B., Bekker, H., Berendsen, H. J. C., & Fraaije, J. G. E. M. (1997). LINCS : A Linear Constraint Solver for Molecular Simulations. *Journal of Computational Chemistry*, *18*(12), 1463–1472. http://doi.org/10.1002/(SICI)1096-987X(199709)18:12<1463::AID-JCC4>3.0.CO;2-H

Holden, J. H., & Czajkowski, C. (2002). Different residues in the GABAA receptor α1T60-α1K70 region mediate GABA and SR-95531 actions. *Journal of Biological Chemistry*, *277*(21), 18785–18792. http://doi.org/10.1074/jbc.M111778200

Hoover, W. G. (1985). Canonical dynamics: Equilibrium phase-space distributions. *Phys. Rev. A*, *31*(3), 1695–1697. http://doi.org/10.1103/PhysRevA.31.1695

Huang, X., Chen, H., Michelsen, K., Schneider, S., & Shaffer, P. L. (2015). Crystal structure of human glycine receptor-α3 bound to antagonist strychnine. *Nature*, *536*, 277–280. http://doi.org/10.1038/nature14972

Jones-Davis, D. M., & Macdonald, R. L. (2003). GABA A receptor function and pharmacology in epilepsy and status epilepticus. *Current Opinion in Pharmacology*, *3*(1), 12–18. http://doi.org/10.1016/S1471-4892(02)00015-2

Kiefer, F., Arnold, K., Künzli, M., Bordoli, L., & Schwede, T. (2009). The SWISS-MODEL Repository and associated resources. *Nucleic Acids Research*, *37*(suppl_1), D387–D392. http://doi.org/10.1093/nar/gkn750

Kittler, J. T., & Moss, S. J. (2003). Modulation of GABA A receptor activity by phosphorylation and receptor trafficking: implications for the efficacy of synaptic inhibition. *Current Opinion in Neurobiology*, *13*, 341–347. http://doi.org/10.1016/S0959-4388(03)00064-3

Kucken, A. M., Teissére, J. a, Seffinga-clark, J., Wagner, D. a, & Czajkowski, C. (2003). Structural requirements for imidazobenzodiazepine binding to GABA(A) receptors. *Molecular Pharmacology*, *63*(2), 289–296. http://doi.org/10.1124/mol.63.2.289

Kucken, A. M., Wagner, D. A., Ward, P. R., Teissére, J. A., Boileau, A. J., & Czajkowski, C. (2000). Identification of Benzodiazepine Binding Site Residues in the gamma2 Subunit of the gamma-Aminobutyric Acid A Receptor. *Molecular Pharmacology*, *57*(5), 932–939.

Lai, P. C., Singer, M. S., & Crasto, C. J. (2005). Structural Activation Pathways from Dynamic Olfactory Receptor-Odorant Interactions. *Chemical Senses*, *30*(9), 781–792. http://doi.org/10.1093/chemse/bji070

Laskowski, R. A., MacArthur, M. W., Moss, D. S., & Thornton, J. M. (1993). PROCHECK: a program to check the stereochemical quality of protein structures. *Journal of Applied Crystallography*, *26*(2), 283–291. http://doi.org/10.1107/S0021889892009944

Malde, A. K., Zuo, L., Breeze, M., Stroet, M., Poger, D., Nair, P. C., … Mark, A. E. (2011). An

automated force field topology builder (ATB) and repository: version 1.0. *Journal of Chemical Theory and Computation*, *7*(12), 4026–4037. http://doi.org/10.1021/ct200196m

Middendorp, S. J., Hurni, E., Schönberger, M., Stein, M., Pangerl, M., Trauner, D., & Sigel, E. (2014). Relative positioning of classical benzodiazepines to the γ2-subunit of GABAA receptors. *ACS Chemical Biology*, *9*(8), 1846–1853. http://doi.org/10.1021/cb500186a

Miller, P. S., & Aricescu, A. R. (2015). Crystal structure of a human GABAA receptor. *Nature*, *512*(7514), 270–275. http://doi.org/10.1038/nature13293

Morley, C. (2016). The Open Babel Package. Retrieved from http://openbabel.org

Morlock, E. V, & Czajkowski, C. (2011). Different residues in the GABAA receptor benzodiazepine binding pocket mediate benzodiazepine efficacy and binding. *Mol Pharmacol*, *80*(1), 14–22. http://doi.org/10.1124/mol.110.069542

Morris, G. M., Huey, R., Lindstrom, W., Sanner, M. F., Belew, R. K., Goodsell, D. S., & Olson, A. J. (2009). AutoDock4 and AutoDockTools4: Automated docking with selective receptor flexibility. *Journal of Computational Chemistry*, *30*(16), 2785–2791. http://doi.org/10.1002/jcc.21256

Moss, S. J., Gorrie, G. H., Amato, A., & Smart, T. G. (1995). Modulation of GABAA receptors by tyrosine phosphorylation. *Nature*, *377*(6547), 344–348. http://doi.org/10.1038/377344a0

Mukherjee, S., Das, S. K., Vaidyanathan, K., & Vasudevan, D. M. (2008). Consequences of alcohol consumption on neurotransmitters-an overview. *Current Neurovascular Research*, *5*(4), 266–272. http://doi.org/10.2174/156720208786413415

Newell, J. G., & Czajkowski, C. (2003). The GABAA receptor Alpha1 subunit Pro174-Asp191 segment is involved in GABA binding and channel gating. *Journal of Biological Chemistry*, *278*(15), 13166–13172. http://doi.org/10.1074/jbc.M211905200

Newell, J. G., McDevitt, R. A., & Czajkowski, C. (2004). Mutation of glutamate 155 of the GABAA receptor β2 subunit produces a spontaneously open channel: a trigger for channel activation. *Journal of Neuroscience*, *24*(50), 11226–11235. http://doi.org/10.1523/JNEUROSCI.3746-04.2004

Nosé, S. (1984). A molecular dynamics method for simulations in the canonical ensemble. *Molecular Physics*, *52*(2), 255–268.

Nutt, D. J., & Malizia, A. L. (2001). New insights into the role of the GABAA-benzodiazepine receptor in psychiatric disorder. *The British Journal of Psychiatry*, *179*(5), 390–396. http://doi.org/10.1192/bjp.179.5.390

Olsson, M. H. M., Søndergaard, C. R., Rostkowski, M., & Jensen, J. H. (2011). PROPKA3: consistent treatment of internal and surface residues in empirical p K a predictions. *Journal of Chemical Theory and Computation*, *7*(2), 525–537.

Oostenbrink, C., Villa, A., Mark, A. E., & Van Gunsteren, W. F. (2004). A biomolecular force field based on the free enthalpy of hydration and solvation: The GROMOS force-field parameter sets 53A5 and 53A6. *Journal of Computational Chemistry*, *25*(13), 1656–1676. http://doi.org/10.1002/jcc.20090

Ortells, M. O., & Lunt, G. G. (1995). Evolutionary history of the ligand-gated ion-channel superfamily of receptors. *Trends in Neurosciences*, *18*(3), 121–127. http://doi.org/http://dx.doi.org/10.1016/0166-2236(95)93887-4

Padgett, C. L., Hanek, A. P., Lester, H. A., Dougherty, D. A., & Lummis, S. C. R. (2007). Unnatural Amino Acid Mutagenesis of the GABAA Receptor Binding Site Residues Reveals a Novel Cation- Interaction between GABA and 2Tyr97. *Journal of Neuroscience*, *27*(4), 886–892. http://doi.org/10.1523/JNEUROSCI.4791-06.2007

Páll, S., Abraham, M. J., Kutzner, C., Hess, B., & Lindahl, E. (2015). Tackling Exascale Software Challenges in Molecular Dynamics Simulations with GROMACS. In S. Markidis & E. Laure (Eds.), *Solving Software Challenges for Exascale: International Conference on Exascale Applications and Software, EASC 2014, Stockholm, Sweden, April 2-3, 2014, Revised Selected Papers* (pp. 3–27). Cham: Springer International Publishing. http://doi.org/10.1007/978-3-319-15976-8_1

Páll, S., & Hess, B. (2013). A flexible algorithm for calculating pair interactions on SIMD architectures. *Computer Physics Communications*, *184*(12), 2641–2650. http://doi.org/http://dx.doi.org/10.1016/j.cpc.2013.06.003

Parrinello, M., & Rahman, A. (1981). Polymorphic transitions in single crystals : A new molecular dynamics method. *Journal of Applied Physics*, *52*(12), 7182–7190. http://doi.org/10.1063/1.328693

Pearson, W. R. (1991). Searching Protein Sequence Libraries : Comparison of the Sensitivity and Selectivity of the Smith-Waterman and FASTA Algorithms. *Genomics*, *11*(3), 635–650.

Retrieved from http://www.sciencedirect.com/science/article/pii/088875439190071L

Pei, J., & Grishin, N. V. (2007). PROMALS: towards accurate multiple sequence alignments of distantly related proteins. *Bioinformatics*, *23*(7), 802–808. http://doi.org/10.1093/bioinformatics/btm017

Puthenkalam, R., Hieckel, M., Simeone, X., Suwattanasophon, C., Feldbauer, R. V., Ecker, G. F., & Ernst, M. (2016). Structural Studies of GABAA Receptor Binding Sites: Which Experimental Structure Tells us What? *Frontiers in Molecular Neuroscience*, *9*(44). http://doi.org/10.3389/fnmol.2016.00044

Raghavan, V., Bollmann, P., & Jung, G. S. (1989). A critical investigation of recall and precision as measures of retrieval system performance. *ACM Transactions on Information Systems (TOIS)*, *7*(3), 205–229.

Richter, L., Graaf, C. De, Sieghart, W., Varagic, Z., Mörzinger, M., Esch, I. J. P. De, … Ernst, M. (2012). Diazepam-bound GABAA receptor models identify new benzodiazepine binding-site ligands. *Nat Chem Biol*, *8*(5), 455–464. http://doi.org/10.1038/nchembio.917.

Rostkowski, M., Olsson, M. H. M., Søndergaard, C. R., & Jensen, J. H. (2011). Graphical analysis of pH-dependent properties of proteins predicted using PROPKA. *BMC Structural Biology*, *11*(1), 6. http://doi.org/10.1186/1472-6807-11-6

Roy, B. C., & Mukherjee, A. (2017). Computational analysis of the glutamate receptor gene family of Arabidopsis thaliana. *Journal of Biomolecular Structure and Dynamics*, *35*(11), 2454–2474. http://doi.org/10.1080/07391102.2016.1222968

Rudolph, U., Crestani, F., Hanns, M., & Rudolph, U. (2001). GABAA receptor subtypes: dissecting their pharmacological functions. *TRENDS in Pharmacological Sciences*, *22*(4), 188–194. http://doi.org/10.1016/S0165-6147(00)01646-1

Saito, T., & Rehmsmeier, M. (2015). The precision-recall plot is more informative than the ROC plot when evaluating binary classifiers on imbalanced datasets. *PloS One*, *10*(3), e0118432. http://doi.org/10.1371/journal.pone.0118432

Sander, T., Frolund, B., Bruun, A. T., Ivanov, I., Mccammon, J. A., & Balle, T. (2011). New insights into the GABA A receptor structure and orthosteric ligand binding: Receptor modeling guided by experimental data. *Proteins: Structure, Function and Bioinformatics*, *79*(5), 1458–1477. http://doi.org/10.1002/prot.22975

Sawyer, G. W., Chiara, D. C., Olsen, R. W., & Cohen, J. B. (2002). Identification of the Bovine γ-Aminobutyric Acid Type A Receptor α Subunit Residues Photolabeled by the Imidazobenzodiazepine [3H] Ro15-4513. *Journal of Biological Chemistry*, *277*(51), 50036–50045. http://doi.org/10.1074/jbc.M209281200

Schüttelkopf, A. W., & van Aalten, D. M. F. (2004). PRODRG: a tool for high-throughput crystallography of protein-ligand complexes. *Acta Crystallographica Section D: Biological Crystallography*, *60*(8), 1355–1363. http://doi.org/10.1107/S0907444904011679

Shen, M., & Sali, A. (2006). Statistical potential for assessment and prediction of protein structures. *Protein Science*, *15*, 2507–2524. http://doi.org/10.1110/ps.062416606

Sieghart, W. (1995). Structure and Pharmacology of gamma-Aminobotyric AcidA Receptor Subtypes. *Pharmacological Reviews*, *47*(2), 182–224.

Sieghart, W., & Sperk, G. (2002). Subunit Composition, Distribution and Function of GABAA Receptor Subtypes. *Current Topics in Medicinal Chemistry*, *2*(8), 795–816. http://doi.org/10.2174/1568026023393507

Sigel, E., & Buhr, A. (1997). The benzodiazepine binding site of GABAA receptors. *Trends in Pharmacological Sciences*, *18*(4), 425–429. http://doi.org/10.1016/S0165-6147(97)90675-1

Simon, J., Wakimoto, H., Fujita, N., Lalande, M., & Barnard, E. A. (2004). Analysis of the Set of GABAA Receptor Genes in the Human Genome. *Journal of Biological Chemistry*, *279*(40), 41422–41435. http://doi.org/10.1074/jbc.M401354200

Smith, G. B., & Olsen, R. W. (1995). Functional domains of GABAA receptors. *TiPS*, *16*(5), 162–168. http://doi.org/10.1016/S0165-6147(00)89009-4

Söding, J., Biegert, A., & Lupas, A. N. (2005). The HHpred interactive server for protein homology detection and structure prediction. *Nucleic Acids Research*, *33*(suppl_2), W244–W248. http://doi.org/10.1093/nar/gki408

Spurny, R., Ramerstorfer, J., Price, K., Brams, M., Ernst, M., Nury, H., … Ulens, C. (2012). Pentameric ligand-gated ion channel ELIC is activated by GABA and modulated by benzodiazepines. *Proceedings of the National Academy of Sciences of the United States of America*, *109*(44), E3028-34. http://doi.org/10.1073/pnas.1208208109

Sternbach, L. H. (1979). The benzodiazepine story. *Journal of Medicinal Chemistry*, *22*(1), 1–7.

http://doi.org/10.1021/jm00187a001

Tan, K. R., Baur, R., Charon, S., Goeldner, M., & Sigel, E. (2009). Relative positioning of diazepam in the benzodiazepine-binding-pocket of GABAA receptors. *Journal of Neurochemistry*, *111*(5), 1264–1273. http://doi.org/10.1111/j.1471-4159.2009.06419.x

Tan, K. R., Gonthier, A., Baur, R., Ernst, M., Goeldner, M., & Sigel, E. (2007). Proximity-accelerated chemical coupling reaction in the benzodiazepine-binding site of γ-aminobutyric acid type A receptors: Superposition of different allosteric modulators. *Journal of Biological Chemistry*, *282*(36), 26316–26325. http://doi.org/10.1074/jbc.M702153200

Teissére, J. A., & Czajkowski, C. (2001). A (beta)-strand in the (gamma)2 subunit lines the benzodiazepine binding site of the GABA A receptor: structural rearrangements detected during channel gating. *The Journal of Neuroscience : The Official Journal of the Society for Neuroscience*, *21*(14), 4977–4986. Retrieved from http://www.ncbi.nlm.nih.gov/pubmed/11438573

Thompson, A. J., Lester, H. a, & Lummis, S. C. R. (2010). *The structural basis of function in Cys-loop receptors. Quarterly reviews of biophysics* (Vol. 43). http://doi.org/10.1017/S0033583510000168

Tretter, V., Ehya, N., Fuchs, K., & Sieghart, W. (1997). Stoichiometry and Assembly of a Recombinant GABA A Receptor Subtype, *17*(8), 2728–2737.

Trott, O., & Olson, A. J. (2010). AutoDock Vina: Improving the speed and accuracy of docking with a new scoring function, efficient optimization, and multithreading. *Journal of Computational Chemistry*, *31*(2), 455–461. http://doi.org/10.1002/jcc.21334

Van Zundert, G. C. P., Rodrigues, J. P. G. L. M., Trellet, M., Schmitz, C., Kastritis, P. L., Karaca, E., … Bonvin, A. M. J. J. (2016). The HADDOCK2.2 Web Server: User-Friendly Integrative Modeling of Biomolecular Complexes. *Journal of Molecular Biology*, *428*(4), 720–725. http://doi.org/10.1016/j.jmb.2015.09.014

Venkatachalan, S. P., & Czajkowski, C. (2008). A conserved salt bridge critical for GABA(A) receptor function and loop C dynamics. *Proceedings of the National Academy of Sciences of the United States of America*, *105*(36), 13604–13609. http://doi.org/10.1073/pnas.0801854105

Vijayan, R. S. K., Bhattacharyya, D., & Ghoshal, N. (2012). Deciphering the binding mode of Zolpidem to GABA(A) α1 receptor - insights from molecular dynamics simulation. *Journal of Molecular Modeling*, *18*(4), 1345–54. http://doi.org/10.1007/s00894-011-1142-0

Vogt, K. (2015). *Diversity in GABAergic Signaling*. *Advances in Pharmacology* (1st ed., Vol. 73). Elsevier Inc. http://doi.org/10.1016/bs.apha.2014.11.009

Wagner, D. A., & Czajkowski, C. (2001). Structure and dynamics of the GABA binding pocket: A narrowing cleft that constricts during activation. *The Journal of Neuroscience*, *21*(1), 67–74.

Wang, S., Liu, Q., Li, X., Zhao, X., Qiu, L., & Lin, J. (2017). Possible binding sites and interactions of propanidid and AZD3043 within the γ-aminobutyric acid type A receptor (GABAAR). *Journal of Biomolecular Structure and Dynamics*, *0*(November), 1–12. http://doi.org/10.1080/07391102.2017.1403959

Webb, B., & Sali, A. (2002). Comparative Protein Structure Modeling Using MODELLER. In *Current Protocols in Protein Science* (p. 5.6.1-5.6.37). John Wiley & Sons, Inc. http://doi.org/DOI: 10.1002/cpbi.3

Westh-Hansen, S. E., Witt, M. R., Dekermendjian, K., Liljefors, T., Rasmussen, P. B. ., & Nielsen, M. (1999). Arginine residue 120 of the human GABA A receptor alpha 1 , subunit is essential for GABA binding and chloride ion current gating. *Neuropharmacology*, *10*(11), 2417–2421.

Wiederstein, M., & Sippl, M. J. (2007). ProSA-web: interactive web service for the recognition of errors in three-dimensional structures of proteins. *Nucleic Acids Research*, *35*(suppl_2), W407–W410. http://doi.org/10.1093/nar/gkm290

Xie, H. B., Sha, Y., Wang, J., & Cheng, M. S. (2013). Some insights into the binding mechanism of the GABAA receptor: A combined docking and MM-GBSA study. *Journal of Molecular Modeling*, *19*(12), 5489–5500. http://doi.org/10.1007/s00894-013-2049-8

Yee, B. K., Keist, R., Von Boehmer, L., Studer, R., Benke, D., Hagenbuch, N., … others. (2005). A schizophrenia-related sensorimotor deficit links α3-containing GABAA receptors to a dopamine hyperfunction. *Proceedings of the National Academy of Sciences of the United States of America*, *102*(47), 17154–17159.

Young, A. B., & Chu, D. (1990). Distribution of GABAA and GABAB Receptors in Mammalian

Brain: Potential Targets for Drug Development. *Drug Development Research*, *21*, 161–167. http://doi.org/10.1002/ddr.430210303

Zhang, J., Xue, F., Liu, Y., Yang, H., & Wang, X. (2013). The structural mechanism of the cys-loop receptor desensitization. *Molecular Neurobiology*, *48*(1), 97–108. http://doi.org/10.1007/s12035-013-8420-z

Supplementary information - Orthosteric and benzodiazepine cavities of the $\alpha_1\beta_2\gamma_2$ $GABA_A$ receptor: Insights from experimentally-validated *in silico* methods.

Methods

The Recall and Precision coefficients are defined as relations between True Positives (TP), False Positives (FP) and False Negatives (FN).

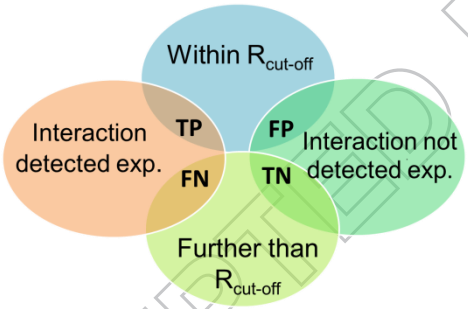

Figure S1. Scheme representing the classification of the interactions between the ligands and the receptor. $R_{cut-off}$ is defined in this work as 2.75Å.

Analysis of the model

Table S1. Qmean and z-scores obtained for the model, the crystallized structure and a previous model (Bergmann, Kongsbak, Sørensen, Sander, & Balle, 2013) showing that the structure of our modelled receptor has good quality.

Structure	Qmean score	Z-score
Our model	0.572	-2.11
4COF	0.581	-2.04
Previous model	0.507	-2.88

Table S2. G-factors of stereochemical parameters analysed with Procheck also show that our modelled receptor maintains an overall good structure. Procheck calculates these values based on an analysis of 163 non-homologous, high-resolution protein chains selected from structures solved by X-ray crystallography to a resolution of 2.0Å or better and an *R*-factor smaller than 20%.

Parameter	G-factor
Phi-psi distribution	0.11
Chi1-Chi2	0.22
Chi1 only	0.34
Chi3 and Chi4	0.54
Omega	-0.13
Overall average	**0.03**

From visual inspection, the chosen model represents correctly both the secondary and tertiary structure of the receptor. The root mean square deviation (RMSD) was calculated for each chain with respect to the crystallographic structure of the template, resulting in an average of 0.15 ± 0.03 Å.

In addition, we measured with HOLE software (Smart, Neduvelil, Wang, Wallace, & Sansom, 1996) the pore profile along the z axis. The analysis of the central pore (Fig. 5) showed that there is a constriction of 1.5 Å delimited by the M2 helices residues α_1Pro240, β_2Ala239 and γ_2Pro239. With this radius no chloride ions can permeate through the channel (r_{os}~4 Å) confirming that our modelled structure is in a closed state (Miller & Aricescu, 2015).

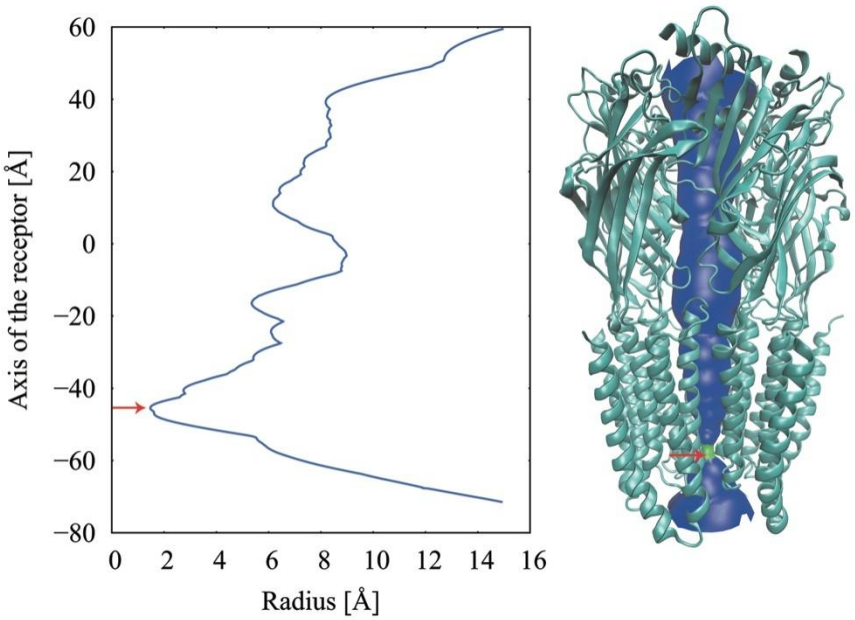

Figure S2. The channel shows a constriction on the lower part of the transmembrane domain, which is in agreement with a desensitized state, in contraposition to an inactive-closed state that displays the constriction in the upper region of the TMD (Hilf & Dutzler, 2008; Miller & Aricescu, 2015; Unwin, 2005).

Employing homology models in molecular docking simulations

It has been subject of debate whether homology models are adequate to be employed in molecular docking studies (both of proteins and small ligands). For data-driven docking experiments, the global folding and the reliability on the information used to guide the docking are the most important aspects for obtaining good predictions (Rodrigues et al., 2013). When the docking is not guided by experiment, it has been shown that the sequence identity, in particular the local sequence identity, is highly correlated with the quality of the docking results (Bordogna, Pandini, & Bonati, 2011); therefore, we calculated the sequence identity for the six loops involved in the binding cavities.

Table S3. Local sequence identity between the template (PDB ID: 4COF) and the α_1, β_2 and γ_2 subunits.

Loop	**α_1**	**β_2**	**γ_2**
Loop A	60%*	100%**	60%
Loop B	50%*	100%**	62.5%
Loop C	33%*	66%**	25%
Loop D	40%**	80%	40%*
Loop E	46%**	100%	53.8%*

Loop F	30%**	77%	22%*

*Loops involved in the benzodiazepines binding cavity

**Loops involved in the orthosteric binding cavity.

Even though loop F of the γ_2 subunit has low (<30%) sequence similarity, it does not contain gaps in the alignment. The other loops involved in the binding show at least 30% of sequence identity with the template, giving more confidence to the docking results. These differences in the primary structure are consistent with a specificity of the compounds that bind to each binding site.

Orthosteric binding site.

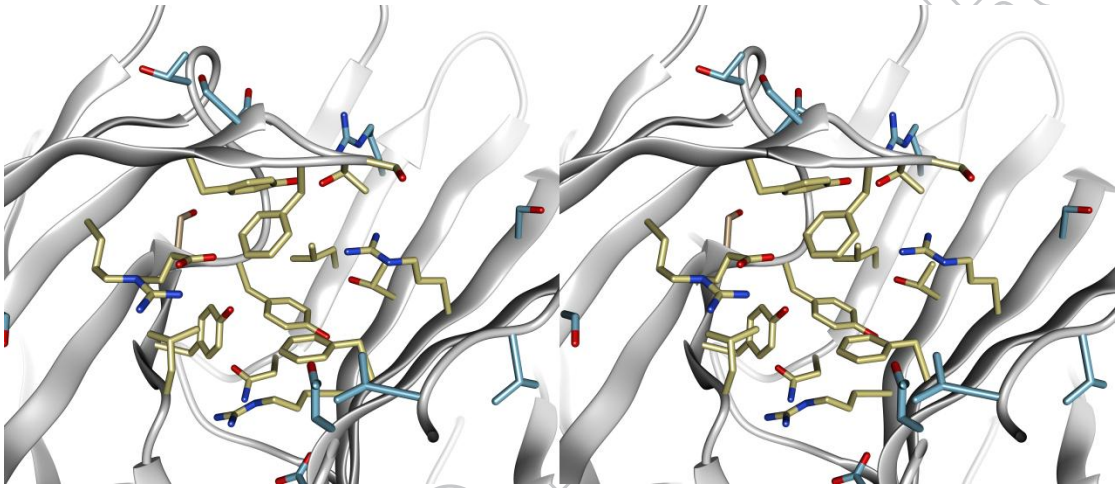

Figure S3. Stereoscopic view of the orthosteric cavity. Amino acids which have been found to form the binding site are represented by lines: those that are in the core of the site according to our model are highlighted in colour khaki, while the ones lining the cavity are in light blue.

Table S4. Experimentally-suggested interactions between ligands and residues of the orthosteric binding cavity.

Loop	Residue	Role	Source
A	β_2Y97	• Cation-π interaction with GABA • SCAM studies show that it is part of the binding site. • Its mutation reduces the sensitivity towards GABA and gabazine.	(Boileau, Newell, & Czajkowski, 2002; Padgett, Hanek, Lester, Dougherty, & Lummis, 2007)
	β_2L99	• SCAM studies show it is part of the binding site, although it might not interact directly with GABA.	(Boileau et al., 2002)
B	β_2E155	• Its mutation affects channel gating and weakens the binding of agonists.	(Newell, McDevitt, & Czajkowski, 2004)

		• Interaction with the amino group of GABA (in sílico model).	
	β_2S156	• Hypothetic H-bond with GABA. • Its mutation reduces the sensitivity towards GABA and gabazine.	(Newell et al., 2004)
	β_2Y157	• It is not proposed to interact via cation-π, but through its hydroxyl group. • Its mutation decreases apparent affinity/sensitivity of GABA and muscimol. Might interact with the carboxyl-like 3-isoxazole moiety of muscimol. • When mutated to Serine, bicuculline and gabazine act as partial agonists.	(Amin & Weiss, 1993; Padgett et al., 2007)
	β_2G158	• Mutation reduces the affinity for GABA and gabazine.	(Newell et al., 2004)
	β_2T160	• Its mutation decreases apparent affinity/sensitivity of GABA and muscimol. • SCAM studies show it is part of the binding site and participates in channel gating.	(Amin & Weiss, 1993; Newell et al., 2004)
	β_2D163	• SCAM studies show it is part of the binding site and participates in channel gating.	(Newell et al., 2004)
C	β_2F200	• Its mutation affects the binding of gabazine and GABA, and the activation of the channel.	(Wagner & Czajkowski, 2001)
	β_2S201	• Its mutation reduces the sensitivity towards GABA and gabazine.	(Wagner & Czajkowski, 2001)
	β_2T202	• Its mutation deactivates the channel. • Its mutation decreases apparent affinity/sensitivity of GABA and muscimol. • Its mutation reduces the sensitivity towards GABA and gabazine.	(Amin & Weiss, 1993; Wagner & Czajkowski, 2001)
	β_2G203	• Its mutation reduces the sensitivity towards GABA and gabazine.	(Wagner & Czajkowski, 2001)
	β_2S204	• SCAM studies show it lines and faces into the binding site. Its mutation did not affect binding affinity of either GABA or gabazine.	(Wagner & Czajkowski, 2001)
	β_2Y205	• Its mutation decreases apparent affinity/sensitivity of GABA, muscimol, bicuculline and gabazine.	(Amin & Weiss, 1993; Padgett et al., 2007; Wagner & Czajkowski,

		• SCAM studies show it lines and faces into the binding site.	2001)
	β2R207	• Mutation causes a decrease in GABA and agonists binding, but not gabazine. • Proposed to stabilize the antagonists binding. • Not involved in the gating process. • SCAM studies show it lines and faces into the binding site.	(Goldschen-Ohm, Wagner, & Jones, 2011; Wagner & Czajkowski, 2001; Wagner, Czajkowski, & Jones, 2004)
	β_2S209	• SCAM studies show it lines and faces into the binding site. It did not affect binding affinity of either GABA or gabazine.	(Wagner & Czajkowski, 2001)
D	α_1D63	• SCAM studies show that gabazine protects this residue, but not GABA.	(Boileau, Evers, Davis, & Czajkowski, 1999)
	α_1F65	• Identified as part of the binding site by SCAM studies. • Photoaffinity labelling of this residue shows that it reacts with the carboxylate-like part of muscimol. • Mutation studies show decreased binding affinity for agonists and antagonists (GABA, bicuculline, gabazine).	(Boileau et al., 1999; Holden & Czajkowski, 2002; Sigel, Baur, Kellenberger, & Malherbe, 1992), (Smith & Olsen, 1994)
	α1R67	• Forms part of the binding cavity (Photoaffinity labelling, SCAM). • It is conserved in all $GABA_A$ receptor α, π and ρ subunits. • Proposed as the anchor of the carboxyl group of GABA. • Its mutation causes a decrease in the binding of GABA and other agonists. • Proposed to obstruct the binding of antagonists. • It is not involved in the gating process.	(Boileau et al., 1999; Goldschen-Ohm et al., 2011; Holden & Czajkowski, 2002)
	α_1S69	• Identified as part of the binding site by SCAM studies.	(Boileau et al., 1999; Holden & Czajkowski, 2002)
E	α1N116	• SCAM studies predict it lines the binding site.	(Kloda & Czajkowski, 2007)
	α1L118	• SCAM studies predict it lines the binding site.	(Kloda & Czajkowski, 2007)
	α1R120	• SCAM studies predict it lines the binding	(Kloda & Czajkowski, 2007;

		site. • Its mutation reduces the binding affinity of muscimol and gabazine, and produces a loss in sensitivity to GABA.	S. E. Westh-Hansen et al., 1999)
	α1I121	• SCAM studies predict it lines the binding site. • Its mutation reduces the sensitivity to GABA and muscimol, but not bicuculline.	(Svend Erik Westh-Hansen et al., 1997)
	α1T130	• SCAM studies predict it lines the binding site.	(Kloda & Czajkowski, 2007)
	α1R132	• SCAM studies predict it lines the binding site. • Its mutation causes a decrease in GABA binding. • Proposed to stabilize the binding of antagonists. • Involved in the gating process.	(Goldschen-Ohm et al., 2011; Kloda & Czajkowski, 2007; Wagner et al., 2004)
F	α_1V179	• SCAM studies show it is part of the binding site, although it might not interact directly with GABA.	(Newell & Czajkowski, 2003)
	α_1V181	• SCAM studies show it is part of the binding site, although it might not interact directly with GABA.	(Newell & Czajkowski, 2003)
	α_1D184	• SCAM studies show it is part of the binding site, although it might not interact directly with GABA.	(Newell & Czajkowski, 2003)

SCAM: substituted cysteine accessibility method.

It is important to note, that relevant residues from the orthosteric site have their analogues in the high affinity benzodiazepines binding site; for example β_2Tyr157 and α_1Tyr159, β_2Tyr205 and α_1Tyr209.

High affinity benzodiazepines binding cavity

We calculated the Tanimoto coefficients for the ligands of the high affinity benzodiazepines binding site. This coefficient can be related to resemblance in binding and function. Such coefficient is defined as: $T_C(A,B)=\frac{c}{a+b-c}$. Where c is the number of features A and B share, and a and b are the number of features present in each compound (Maggiora, Vogt, Stumpfe, & Bajorath, 2014). This coefficient is considered one of the best metrics for similarity calculation.

Classical benzodiazepines share high similarity, which is reflected in the high Tanimoto indexes between them. On the other hand, imidazo-benzodiazepines show high similarity between them, but very low compared to classical benzodiazepines, confirming there is a

substantial difference between these molecules and their expected binding modes. Despite being agonists, Zolpidem and Eszopiclone display very low Tanimoto indexes, which are expected because of the prominent different geometry.

Figure S4. Tanimoto coefficient for the ligands of the benzodiazepines binding site

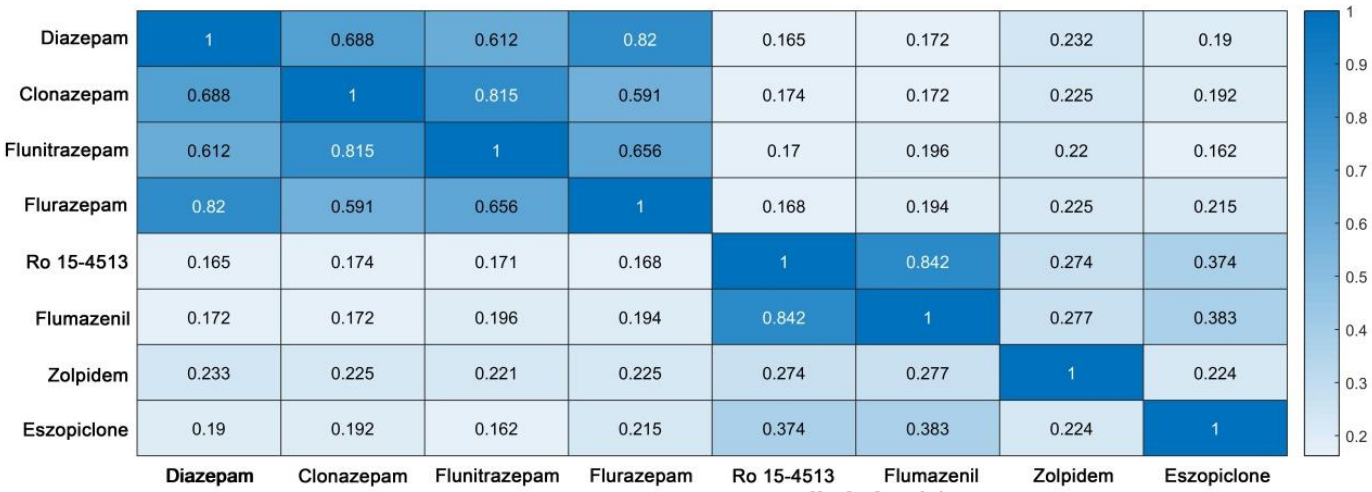

employed in this work.

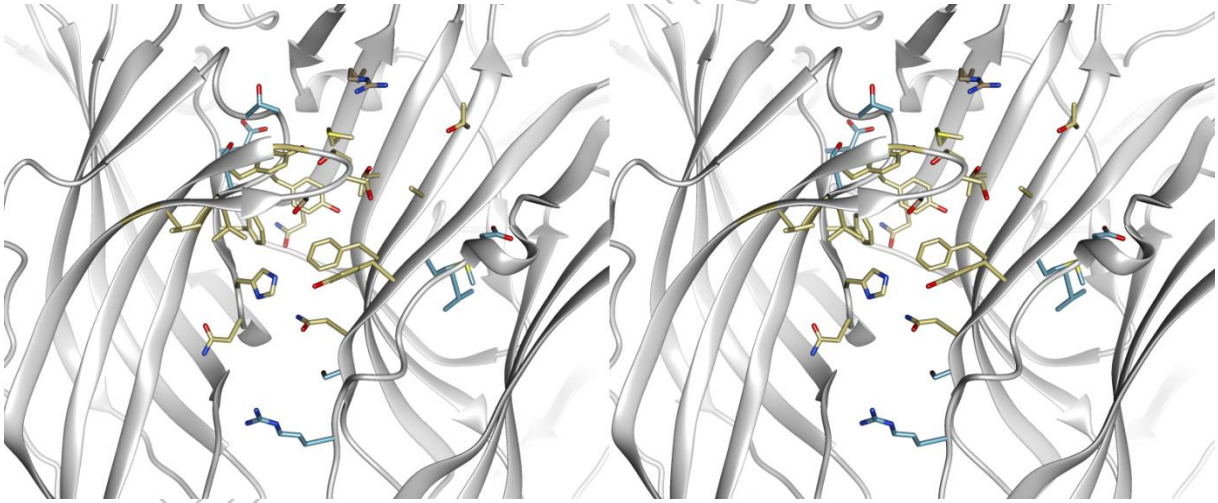

Figure S5. Stereoscopic view of the high affinity benzodiazepine binding cavity. Residues that have been identified as part of the binding site are depicted with licorice: in colour khaki those that form the core of the site and in light blue those that, according to our model, only line the cavity.

Table S5: Summary of the experimental information concerning the amino acids that are putatively involved in the interaction with ligands, or that are an important part of the binding site.

Loop	Residue	Role	Source

A	α1D98	• Mutation studies have shown it affects both the binding and efficacy of agonists, as well as binding of flumazenil.	(Hanson, Morlock, Satyshur, & Czajkowski, 2008; Morlock & Czajkowski, 2011)
	α1F100	• Mutations studies have shown it affects both binding and efficacy of agonists. • Involved in π-π stacking. • Its mutation to cysteine, switches the action of eszopiclone and diazepam from positive allosteric modulators to negative modulators, but it does not affect the binding of flumazenil. It reduces the binding affinity of zolpidem and eszopiclone. • It has been proposed that, if mutated, this amino acid can interfere with the spatial disposition of the side chains of α_1His102 and α_1Tyr160.	(Hanson et al., 2008; Morlock & Czajkowski, 2011; Tan, Baur, Gonthier, Goeldner, & Sigel, 2007)
	α1H102	• SCAM studies have shown that the chlorine atom of diazepam points towards this residue. • It is photolabelled by flunitrazepam. • Identified through domain exchange and site-directed mutagenesis as necessary for the binding of diazepam and zolpidem. • Its mutation to arginine decreases the binding of flumazenil but does not affect Ro15-4513 (i-BDZs bind to receptors formed by α4 and α6 subunits). • Its mutation decreases the binding affinity of zopiclone. (The reduction is smallest if mutated to phenylalanine). • The 7-substituent of i-BDZs is nearby this residue. (Proximity-accelerated chemical coupling) • Mutations to arginine cause Ro15-4531 and flumazenil to turn into potent positive modulators (altering efficacy). While making the receptors insensitive to diazepam (altering affinity).	(Benson, Löw, Keist, Mohler, & Rudolph, 1998; Berezhnoy, Nyfeler, Gonthier, Goeldner, & Sigel, 2004; Davies, Newell, Derry, Martin, & Dunn, 2000; Duncalfe, Carpenter, Smillie, Martin, & Dunn, 1996; Middendorp et al., 2014; Tan, Gonthier, et al., 2007; Tan, Baur, Charon, Goeldner, & Sigel, 2009; Wieland & Lüddens, 1994; Wieland, Lüddens, & Seeburg, 1992)
	α1N103	• Studies by proximity-accelerated chemical coupling reaction showed it points into the binding pocket. • It is expected that the chlorine atom of diazepam and 7-substituent of i-BDZs point towards this residue, but it is less accessible than His102. • Its mutation to cysteine does not affect the binding of flumazenil.	(Tan et al., 2009; Tan, Baur, et al., 2007)

B	α1G158	• Mutations studies have shown it affects both binding and efficacy of agonists. • The chlorine atom of diazepam points towards this residue. • The 7-substituent of i-BDZs is nearby this residue. (Proximity-accelerated chemical coupling). • Its mutation to cysteine reduces the binding affinity of Zolpidem and Eszopiclone.	(Hanson et al., 2008; Morlock & Czajkowski, 2011; Tan, Gonthier, et al., 2007; Tan et al., 2009)
	α1S159	• Its mutation to cysteine decreased the binding affinity of flunitrazepam and flumazenil.	(Tan, Gonthier, et al., 2007; Tan et al., 2009)
	α1Y160	• SCAM studies have shown that it lines the binding cavity. • Replacement by serine resulted in the loss of flumazenil and diazepam binding. • Its mutation to cysteine decreased the binding affinity of flunitrazepam and flumazenil.	[17](Amin et al., 1997; Tan, Gonthier, et al., 2007; Tan et al., 2009)
	α1T163	• Mutation studies have shown that it is important for the binding affinity of diazepam. • Its mutation to alanine causes an increase in efficiency of diazepam and zolpidem, and a negligibly increase in the sensitivity of diazepam.	(Buhr, Baur, Malherbe, & Sigel, 1996; Wieland & Lüddens, 1994)
C	α1G201	• Its mutation to cysteine causes a reduction of the binding affinities of flurazepam, eszopiclone and zolpidem. • If mutated to glutamic acid, the affinity of zolpidem is reduced, while the affinity of flumazenil is increased and that of diazepam does not change.	(Hanson et al., 2008; Morlock & Czajkowski, 2011; Pritchett & Seeburg, 1991; Schaerer, Buhr, Baur, & Sigel, 1998; Wieland & Lüddens, 1994)
	α1V203	• The chlorine atom of diazepam points towards this residue. • The 7-substituent of i-BDZs is nearby this residue. (Proximity-accelerated chemical coupling) • Its mutation to cysteine reduces the binding affinity of zolpidem and eszopiclone.	(Hanson et al., 2008; Tan, Gonthier, et al., 2007)
	α1S205	• Its mutation affects the binding affinity of zolpidem.	(Hanson et al., 2008)
	α1S206	• It has been experimentally (proximity-accelerated Chemical coupling) related to C3 atom from the benzodiazepine ring. • Its mutation to alanine does not affect the potentiation of classical benzodiazepines. • Its mutation to asparagine causes a decrease	(Buhr et al., 1996; Derry, Dunn, & Davies, 2004; Middendorp et al., 2014; Tan et al., 2009)

		in the binding affinities of i-BZDs, but not flunitrazepam.	
	α1T207	• It is related to the efficacy of flurazepam, eszopiclone and zolpidem but not to their binding affinity. • It has been experimentally (proximity-accelerated chemical coupling) related to C3 atom from the benzodiazepine ring. • It shares polar contacts with the group N-methyl, which is directed outside the cavity. • Mutation to alanine shows a small decrease in the affinity of flumazenil, diazepam and zolpidem. It also causes an increase in efficiency of diazepam and zolpidem. • Its mutation to valine causes a decrease in the binding affinity of diazepam and zolpidem, and an increase of the binding affinity of flumazenil.	(Buhr et al., 1996; Buhr, Schaerer, et al., 1997; Morlock & Czajkowski, 2011; Schaerer et al., 1998; Sigel, Schaerer, Buhr, & Baur, 1998; Tan et al., 2009)
	α1G208	• Its mutation to cysteine decreases the binding affinity of flunitrazepam and flumazenil.	(Tan, Gonthier, et al., 2007; Tan et al., 2009)
	α1Y210	• Mutations studies have shown it affects both binding and efficacy of agonists. • The aromatic feature is important for the binding of ligands. • Its mutation to glutamine or cysteine abolished the binding affinity for flumazenil and flunitrazepam. • Replacement by phenylalanine causes a reduction of the binding of flumazenil, diazepam and zolpidem, while replacement by serine or alanine an abolition of the binding of these ligands. • Ro15-4513 is photo-incorporated into this residue; it is proposed to react with the azide group.	(Amin et al., 1997; Buhr, Schaerer, et al., 1997; Hanson et al., 2008; Morlock & Czajkowski, 2011), (Sawyer, Chiara, Olsen, & Cohen, 2002)
	α1V212	• When mutated to cysteine it increases the efficacy of zolpidem. • The chlorine atom of diazepam points towards this residue. • The 7-substituent of i-BDZs is nearby this residue. (Proximity-accelerated chemical coupling) • Mutation studies have shown that it is important for flunitrazepam and diazepam, but Ro15-4513 prefers an isoleucine in this position.	(Morlock & Czajkowski, 2011; Tan, Gonthier, et al., 2007; Tan et al., 2009; Wieland & Lüddens, 1994)

β-1 strand	γ2M57	• Mutation studies have shown it is essential for the high-affinity binding of flunitrazepam. • It has been identified as important for the binding of zolpidem.	(Buhr & Sigel, 1997; Kucken et al., 2000)
	γ2Y58	• Mutation studies have shown it is essential for the high-affinity binding of flunitrazepam. • Its mutation to cysteine causes a decrease in the binding affinity of flunitrazepam and diazepam, but not flumazenil. • Through proximity-accelerated chemical coupling reaction, it has been related to C3 atom in the benzodiazepine ring and the 7 substituent.	(Kucken et al., 2000; Middendorp et al., 2014)
	γ2N60	• Its mutation to cysteine causes a slight decrease in the binding affinity of flunitrazepam and diazepam, but not flumazenil. • Through proximity-accelerated chemical coupling reaction, it has been related the 7 substituent of classical benzodiazepines.	(Middendorp et al., 2014)
	γ2S61	• Its mutation to cysteine severely affects the binding of flunitrazepam and abolishes the binding of flumazenil.	(Middendorp et al., 2014)
D	γ2F77	• It is essential for functioning and the binding of flumazenil and clonazepam. • Its mutation to isoleucine resulted in a complete loss of the affinities of zolpidem and flumazenil, while high affinity to flunitrazepam was retained. • Its mutation to cysteine resulted in a complete loss of potentiation by flurazepam, zolpidem, flunitrazepam and flumazenil. • Its mutation to leucine resulted in a complete loss of potentiation and binding of zolpidem, while affinity to diazepam and flumazenil was retained but reduced. • Its mutation to tyrosine considerably reduced the binding affinity of diazepam and flunitrazepam, but slightly increased the affinity of zolpidem and had no effect on flumazenil. • Its mutation to tryptophan reduced considerably the binding affinities of flumazenil and diazepam.	(Buhr et al., 1996; Buhr, Baur, & Sigel, 1997; Sigel et al., 1998; Tan et al., 2009; Teissére & Czajkowski, 2001; Wingrove, Thompson, Wafford, & Whiting, 1997)
	γ2A79	• Mutation studies have shown it is important for high-affinity binding of classic benzodiazepines. • Its mutation to cysteine reduces the binding	(Hanson et al., 2008; Kucken et al., 2000; Kucken, Teissére, Seffinga-clark, Wagner,

		affinity of zolpidem and eszopiclone. • Fundamental for the high affinity binding of i-BDZs. SCAM studies showed the 3'substituent of the i-BDZs lies near this residue. • SCAM studies revealed that it lies within the BZDs binding site. • Its mutation to a tyrosine affected the binding of i-BDZs, but not of flunitrazepam.	& Czajkowski, 2003; Teissére & Czajkowski, 2001)
	γ2T81	• Its mutation affects the binding of i-BDZs and classical BDZs to a less extent. • Its mutation to cysteine reduces the binding affinity of zolpidem. • SCAM studies revealed that it lies within the BZD binding site, it is located near the 3'substituent of i-BDZs and flurazepam does not protect it from covalent modification.	(Hanson et al., 2008; Kucken et al., 2000, 2003; Teissére & Czajkowski, 2001)
E	γ2M130	• Its mutation to cysteine causes a reduction of the binding affinities of flurazepam, eszopiclone and zolpidem. Other studies show this mutation increases the binding affinity of zolpidem. • The mutation to leucine leads to a 51-fold loss in the affinity for zolpidem while affinity for diazepam is only slightly reduced. • Mutational studies show it does not affect the binding of flumazenil, but determines the binding of flunitrazepam and clonazepam.	(Buhr & Sigel, 1997; Hanson et al., 2008; Morlock & Czajkowski, 2011; Sigel et al., 1998; Wingrove et al., 1997)
	γ2R132	• Its mutation to cysteine causes a reduction of the binding affinities of flurazepam, eszopiclone and zolpidem. • Other studies show this mutation increases the binding affinity of zolpidem.	(Hanson et al., 2008; Morlock & Czajkowski, 2011)
	γ2T142	• Its mutation to serine causes Ro15-4513 and flumazenil to turn into potent positive modulators. Further potentiation of GABA responses by diazepam, clonazepam, or flunitrazepam doubled in receptors containing this mutation. In contrast, responses to zolpidem were roughly halved.	(Mihic, Whiting, Klein, Wafford, & Harris, 1994)
	γ2R144	• When mutated to cysteine, it reduced the binding affinity of eszopiclone.	(Hanson et al., 2008)
	γ2E189	• When mutated to cysteine, it increased the efficacy of zolpidem.	(Morlock & Czajkowski, 2011)
F	γ2V190	• Although it is not directly in contact with diazepam, it is associated with the orientation of the ligand. • Through proximity-accelerated chemical coupling reaction it was shown that classical	(Middendorp et al., 2014)

		benzodiazepines orient their NCH_3 group towards this residue.	
	γ2R197	• It is related to the efficacy of flurazepam, eszopiclone and zopidem but not to their binding affinity. • Flurazepam and zolpidem significantly slowed its covalent modification, suggesting movements in loop F, after binding.	(Hanson & Czajkowski, 2008; Morlock & Czajkowski, 2011)

Stability of the MD Simulations

We evaluated the root-mean-square deviation (RMSD) of the different complexes throughout the MD simulations and compared their values to the one obtained for the crystallographic structure under the same conditions. All the systems are stable after approximately 60ns and the RSMD never exeeds 0.5 nm.

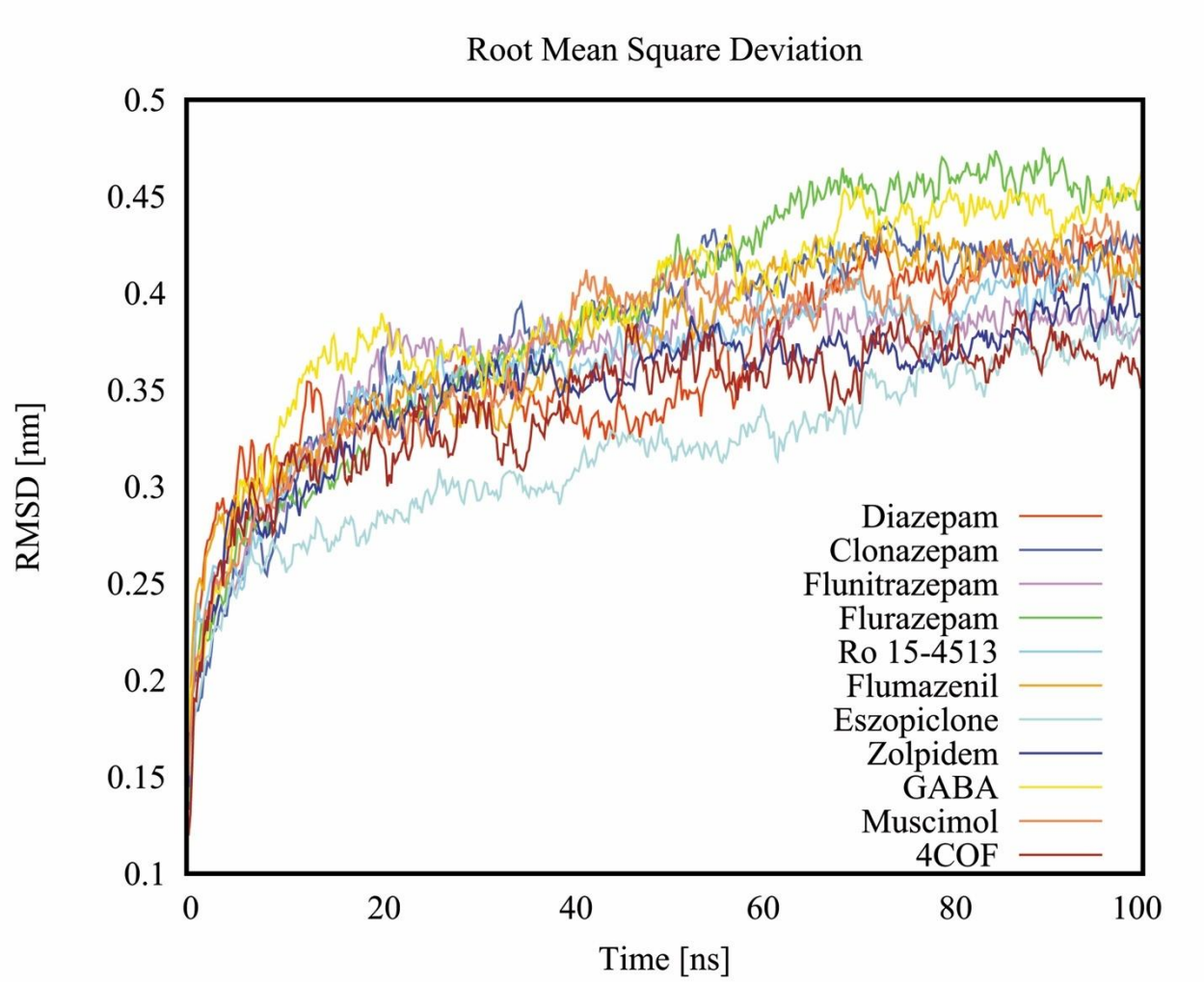

Figure S7. Cα-RMSD plot for the complexes formed by the receptor and the different ligands along the molecular dynamics simulations.

In addition, with the aim of assessing the global movements of the ligands inside the binding cavity we calculated RMSD of the ligands with respect to the initial conformation (Figure S8). Fitting procedures were applied, to rotation and translation, on the protein. The results should highlight the stability of the ligands, a property that has been related to the reliability and accuracy of the predicted complexes (Alonso, Bliznyuk, & Gready, 2006). Flurazempam as well as diazepam display the largest RMSD values due to an initial drastic change in conformation and a subsequent stability, which can be appreciated through the visualization of the trajectory. This initial reorientation might be related to slightly lower values of Recall in comparison with the other ligands. Although they can be considered high, the false positive contacts might account for repulsive forces that lead to the observed movements. The rest of the compounds suffer less changes in their position and orientation inside the cavity and the RMSD values can be related to small movements due to the relaxation of the side chains of the surrounding residues.

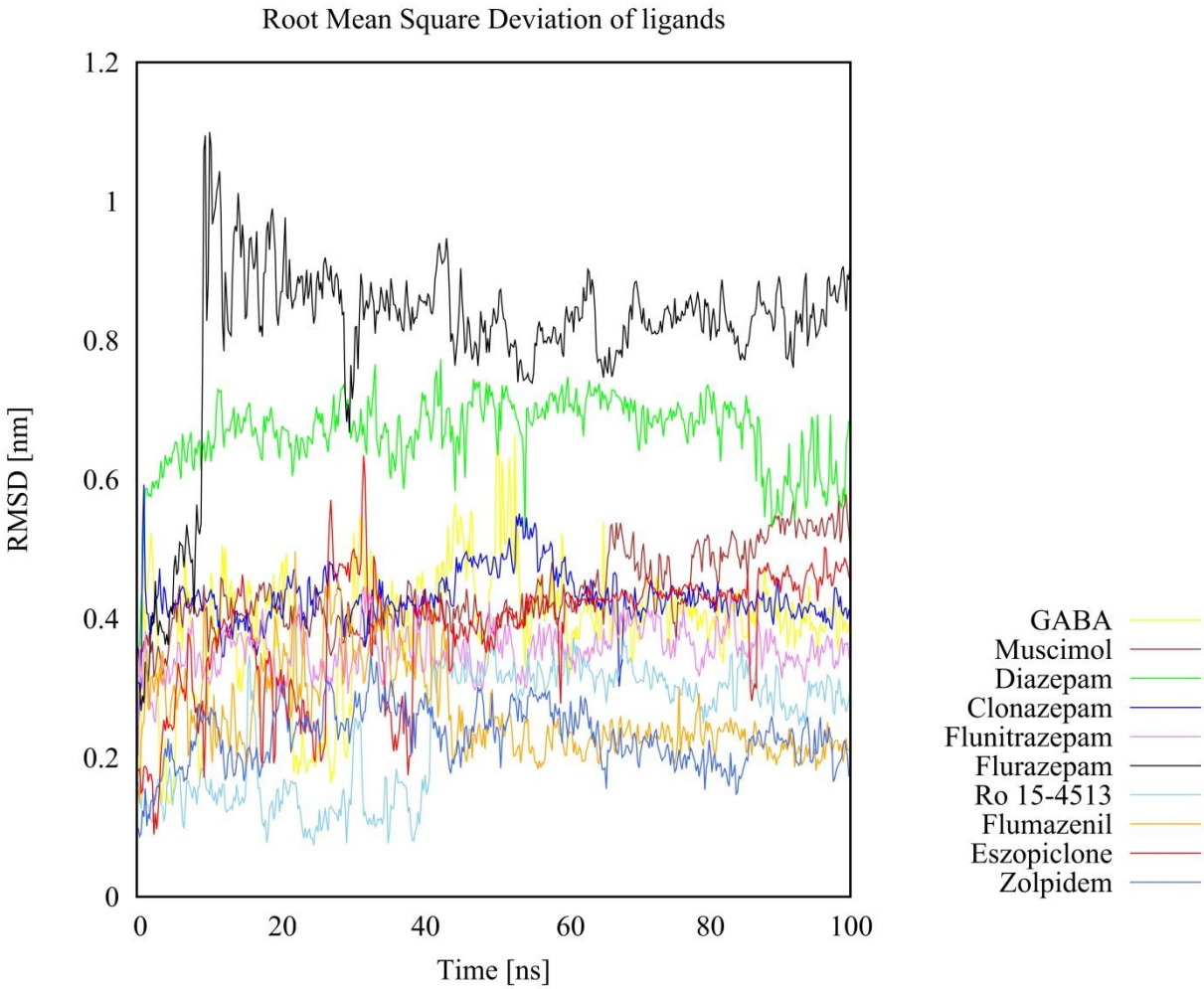

Figure S8. RMSD of the ligands with respect to their initial conformation along the molecular dynamics simulations.

Binding modes obtained from the MD simulations

The binding modes of GABA and muscimol obtained from the MD simulations are depicted in Figures 9 and 10.

As a general feature, the binding poses of the ligands of the orthosteric cavity were improved throughout the MD simulations provided the recall and precision values are considered. Those amino acids involved in the interaction with the ligands were classified as True Positives, False Positives and False Negatives according to the criteria explained in the methods section.

Whereas the binding poses of ligands that were examined through MD simulations do not present False Positive residues, those that have yet to be refined, display a few number of bad contacts due to their large size and lack of reorganization of the side-chains of the surrounding amino acids. Regarding the false negatives for GABA, β_2Ser156 is observed to form an H-bond with the ligand momentarily and therefore cannot be considered as a true positive, although longer simulations might statistically improve the contact. β_2R207 is engaged in an interaction with a residue from loop F (Figure 19) and interacts with β_2Glu155 (Figure 21), thus, even though it is not interacting directly with the ligand it has an active participation in the binding mode.

Table 6. Categorization of residues according to their interaction with the ligands of the orthosteric cavity.

Ligand	**True Positives**	**False Positives**	**False Negatives**
GABA	β_2Tyr97, β_2Glu155, β_2Tyr157, β_2Gly158, β_2Phe200, β_2Ser201, β_2Thr202, β_2Tyr205, α_1Phe65, α_1Arg67, α_1Thr130	-	β_2Ser156, β_2R207
Muscimol	β_2Tyr97, β_2Glu155, β_2Ser156, β_2Tyr157, β_2Phe200, β_2Thr202, β_2Tyr205, β_2Arg207 α_1Phe65, α_1Arg67, α_1Arg120, α_1Thr130	-	-
Bicuculline†	β_2Tyr97, β_2Leu99, β_2Tyr157, β_2Phe200, β_2Thr202, β_2Tyr205, β_2Arg207 α_1Phe65, α_1Arg67, α_1Leu118, α_1Val181	β_2Glu153, β_2Val199 α_1Val180, α_1R120	β_2Ser156, α_1Arg132
Gabazine†	β_2Tyr97, β_2Leu99, β_2Ser156, β_2Tyr157, β_2Phe200, β_2Thr202, β_2Gly203, β_2Tyr205, α_1Phe65, α_1Arg67, α_1Leu118, α_1Thr130, α_1Val181	-	β_2Gly158, β_2Ser201, α_1Asp63, α_1Arg120

† The results here presented for these ligands are obtained from the molecular docking.

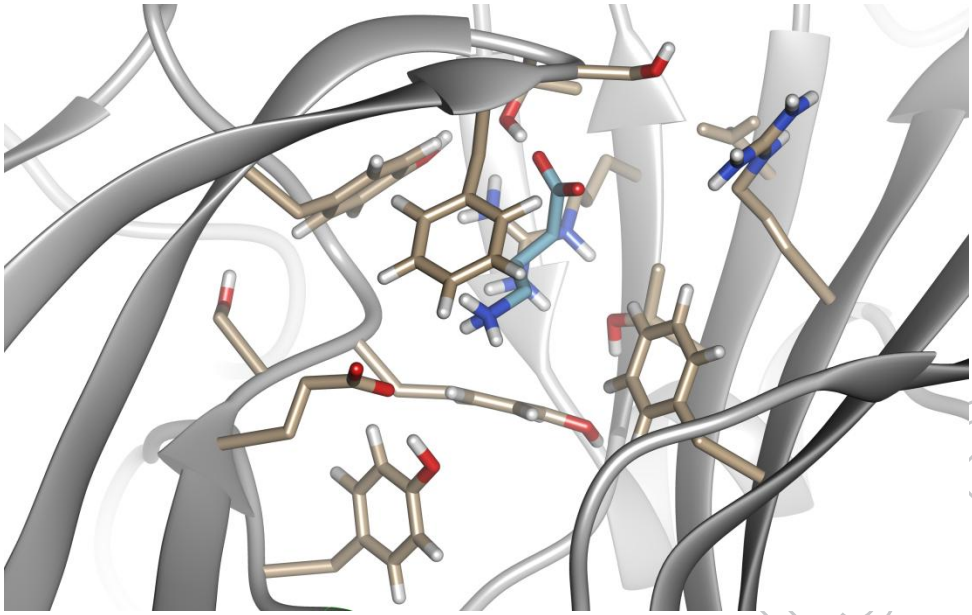

Figure S9. Representation of GABA bound to the model of the $GABA_A$ receptor. The image corresponds to the representative frame after clustering the trajectory obtained from the 100ns MD simulation.

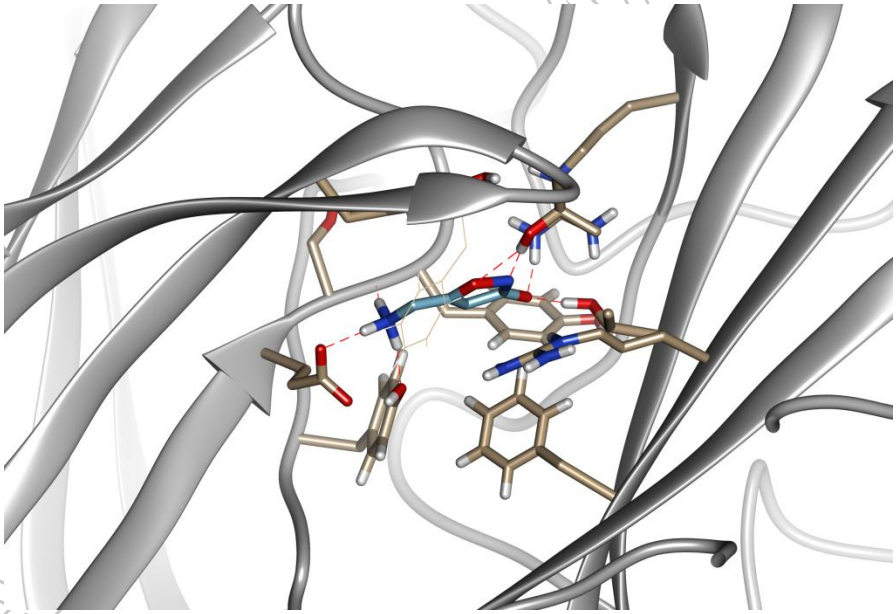

Figure S10. Muscimol is depicted bound to the modelled receptor as in the middle frame of the clustering of the trajectory obtained from their MD simulation.

Regarding the binding poses of the ligands in the benzodiazepines high affinity binding site, we observed that the recall and precision scores were generally increased, except in the simulation of flumazenil. The residues involved in the putative interactions are categorised in

Table 7.

While the binding mode of diazepam does not present false positives, α_1Thr207 and γ_2Ala79 appear far from the ligand; the first due to the opening of the tip of loop C, the latter because of the rearrangement in the orientation of diazepam. However, the interaction of the classical benzodiazepines with γ_2Ala79 is not clear.

The binding mode of clonazepam exhibits a false positive since γ_2Asn60 interacts with the ligand but is not engaged in a natural occurring interaction. Conversely, α_1Ser159 constitutes a false negative since in analogy to the binding of flunitrazepam it should interact with the ligand.

Due to the opening of loop C, α_1Thr207 is not engaged in the predicted interaction with flunitrazepam, while γ_2Ala79 and γ_2Ser61 belong to the binding site, but afar from this ligand.

The binding mode of flurazepam obtained from MD simulations displays γ_2Arg132 within the range of interaction of the ligand but is not engaged in any naturally occurring interaction. On the other hand α_1Gly201, γ_2Ala79, γ_2Met130 are all far from the ligand.

Regarding the amino acids experimentally involved in the binding of Ro15-4513, γ_2Thr81 lies in the model far from the binding site. However, this ligand shows an interaction with γ_2Arg97 in the pose obtained by MD simulations, which is not experimentally predicted to interact with the ligand. The abundance of bad contacts of flumazenil has been related to an initial bad conformation.

Neither zolpidem nor eszopiclone exhibit false positives. However, both display two false negatives: γ_2Thr81, γ_2Met130 for the former and, γ_2Arg132 and γ_2Arg144 for the latter. The absence of contact with γ_2Met130 is mainly due to the movement of the ligand inside the cavity and the relaxation of the side chains of the surrounding amino acids, since it was initially involved in the binding. As has been observed for previous ligands γ_2Thr81 is not modelled inside the binding site in our receptor. γ_2Arg132 and γ_2Arg144 lie in the upper and lower sides of the cavity respectively; they are engaged in other interactions but are not close enough to the ligand to interact with it. Mutating these ligands to a cysteine might cause changes in the binding site, rather than impeding the binding itself.

Table 7. Classification of residues according to their interaction with the ligands of the benzodiazepines binding cavity.

Ligand	True Positives	False Positives	False Negatives
Diazepam	α_1Phe100, α_1His102, α_1Asn103, α_1Tyr160, α_1Val203, α_1Ser206, α_1Tyr210, α_1Val212, γ_2Tyr58, γ_2Asn60,γ_2Phe77, γ_2Ala79, γ_2Arg132	-	α_1Thr207, γ_2Ala79
Clonazepam	α_1Phe100, α_1His102, α_1Gly158, α_1Tyr160, α_1Val203, α_1Ser206, α_1Thr207, α_1Gly208, α_1Tyr210, α_1Val212, γ_2Tyr 58, γ_2Phe77, γ_2Ala79, γ_2Met130, γ_2Thr142	γ_2Asn60	α_1Ser159
Flunitrazepam	α_1Phe100, α_1His102, α_1Ser159, α_1Tyr160, α_1Val203, α_1Ser205, α_1Tyr210, α_1Val212, γ_2Tyr 58, γ_2Asn60, γ_2Phe77, γ_2Met130, γ_2Arg132, γ_2Thr142	α_1Thr207,	γ_2Ala79, γ_2Ser61
Flurazepam	α_1Phe100, α_1His102, α_1Ser159, α_1Tyr160, α_1Val203, α_1Ser205, α_1Thr207 α_1Tyr210, α_1Val212, γ_2Tyr 58, γ_2Asn60, γ_2Phe77, , γ_2Thr142	γ_2Arg132	α_1Gly201, γ_2Ala79, γ_2Met130
Ro15-4513	α_1Phe100, α_1His102, α_1Gly158, α_1Ser159, α_1Tyr160, α_1Val203, α_1Ser205, α_1Ser206, α_1Thr207 α_1Tyr210, α_1Val212, γ_2Tyr58, γ_2Phe77, γ_2Ala79, γ_2Met130, γ_2Thr142	γ_2Arg97	γ_2Thr81
Flumazenil	α_1His102, α_1Tyr160, α_1Val203, α_1Ser205, α_1Thr207 α_1Tyr210, α_1Val212, γ_2Tyr58, γ_2Phe77, γ_2Ala79, γ_2Thr142	α_1Lys155, γ_2Asp56, γ_2Arg132	α_1Ser159, α_1Ser206, γ_2Ser61, γ_2Thr81
Zolpidem	α_1Phe100, α_1His102, α_1Gly158, α_1Ser159, α_1Tyr160, α_1Val203, α_1Ser206, α_1Thr207 α_1Tyr210, α_1Val212, γ_2Tyr58, γ_2Phe77, γ_2Ala79, γ_2Thr142	-	γ_2Thr81, γ_2Met130

Eszopiclone	α_1Phe100, α_1His102, α_1Gly158, α_1Ser159, α_1Tyr160, α_1Val203, α_1Ser206, α_1Tyr210, α_1Val212, γ_2Tyr58, γ_2Phe77, γ_2Ala79, γ_2Met130, γ_2Thr142	-	γ_2Arg132, γ_2Arg144

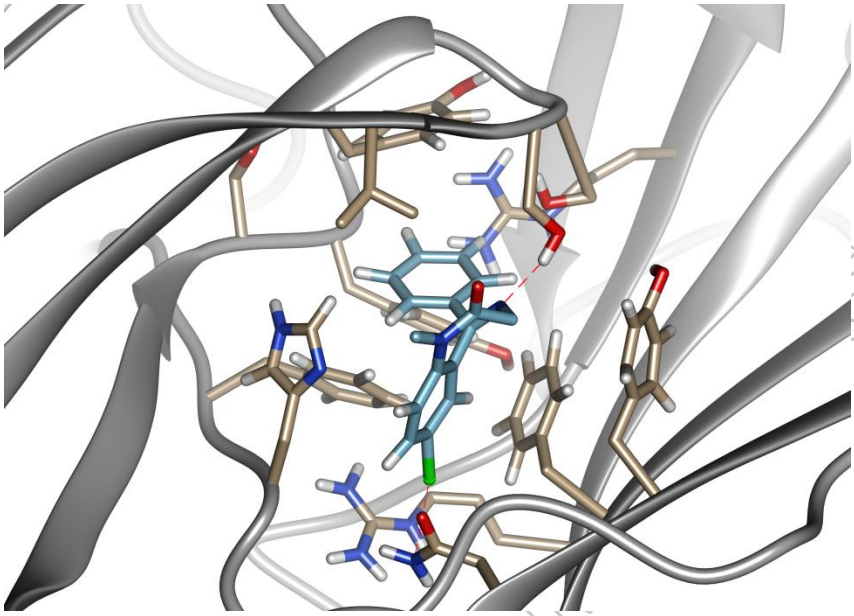

Figure S11. Diazepam bound to the model of the $GABA_A$ receptor taken from the middle frame after clustering of the 100ns MD simulation.

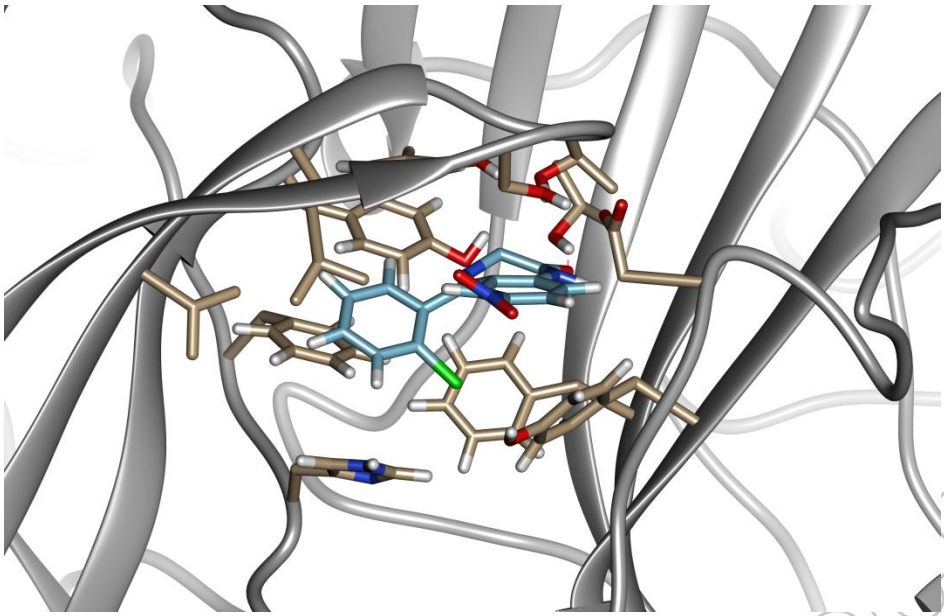

Figure S12. Representative frame of the trajectory of the MD simulation of clonazepam bound to the modelled receptor.

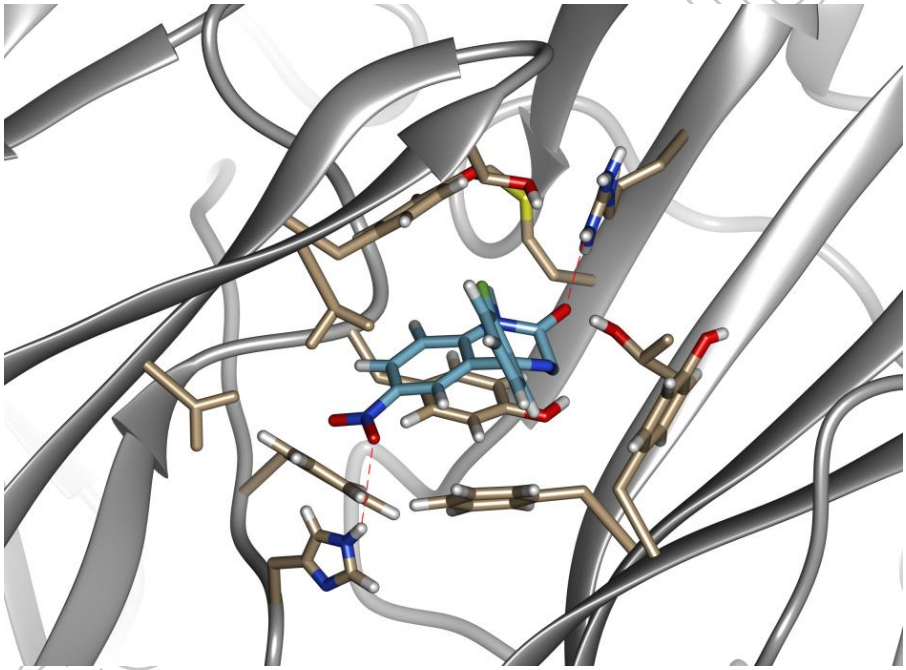

Figure S13. Flunitrazepam is depicted while bound to the modelled receptor in the middle frame of the clustering of the trajectory of the MD simulation.

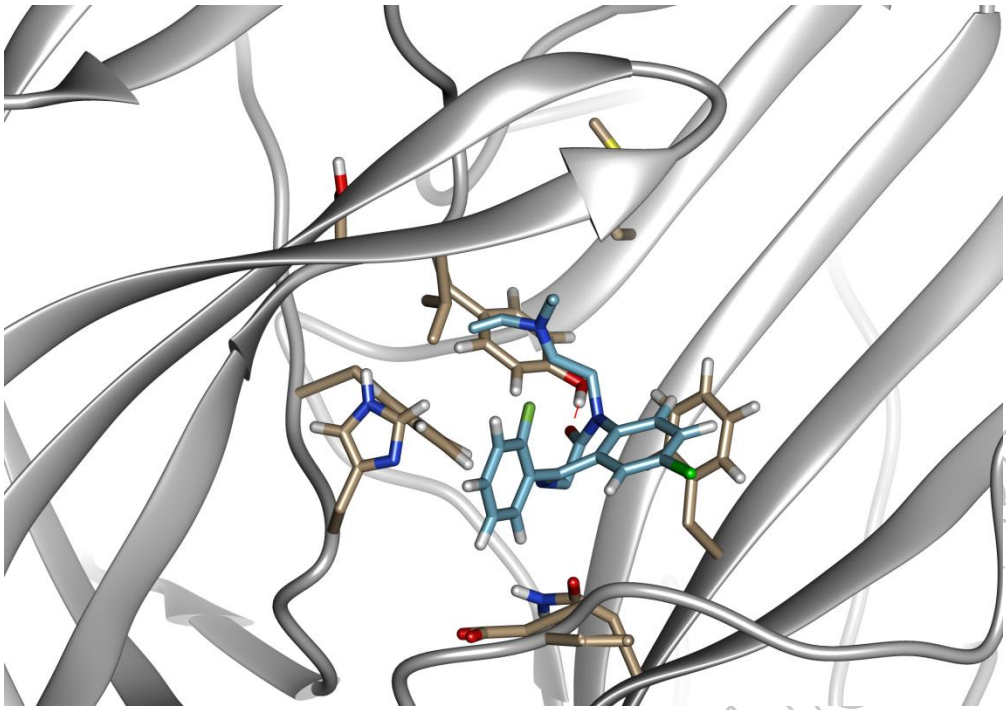

Figure S14. Flurazepam bound to the model of the $GABA_A$ receptor taken from the middle frame after clustering of the 100ns MD simulation.

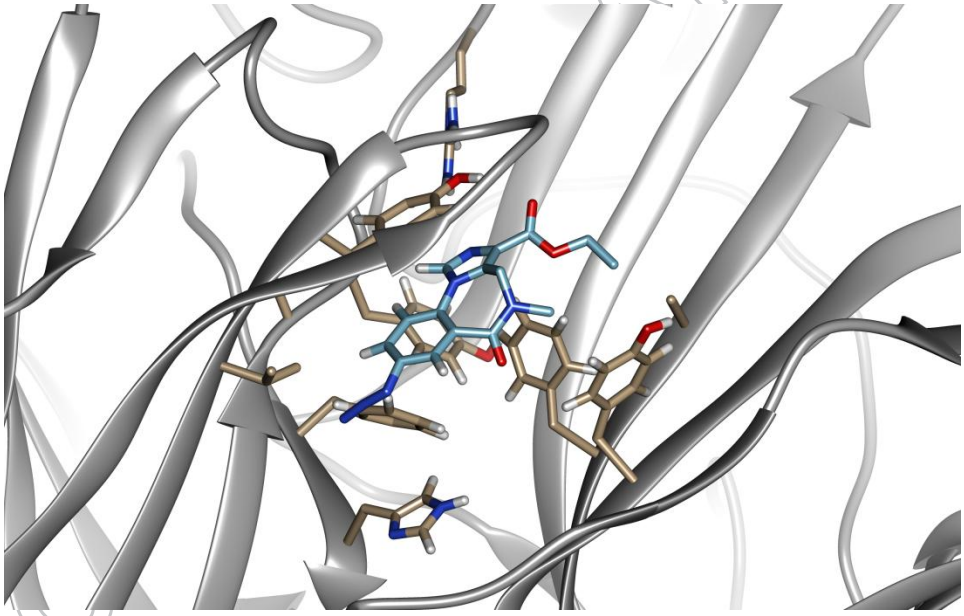

Figure S15. Ro154513 bound to the model of the $GABA_A$ receptor taken from the middle frame after clustering of the 100ns MD simulation.

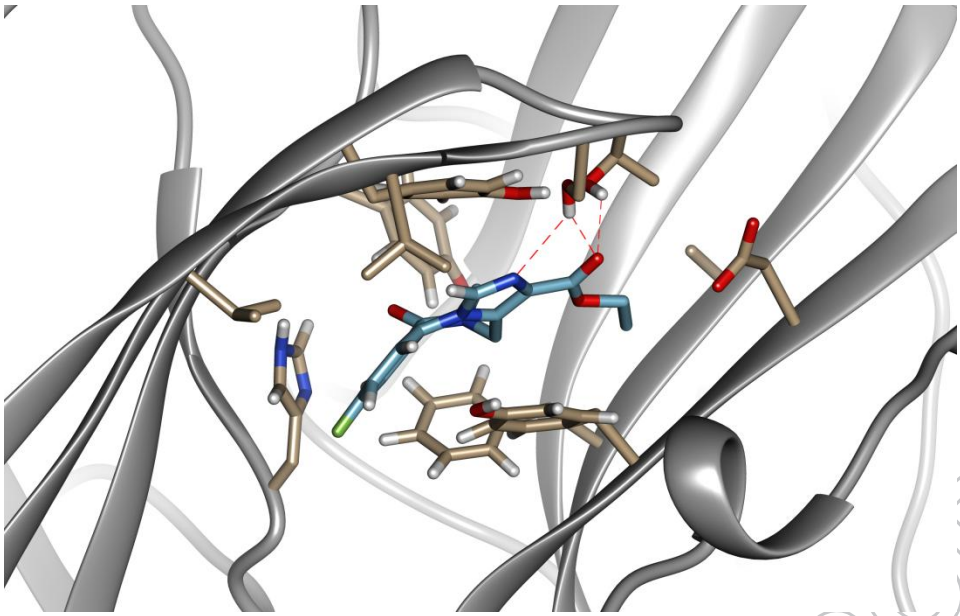

Figure S16. Flumazenil is depicted while bound to the modelled receptor in the middle frame of the clustering of the MD simulation.

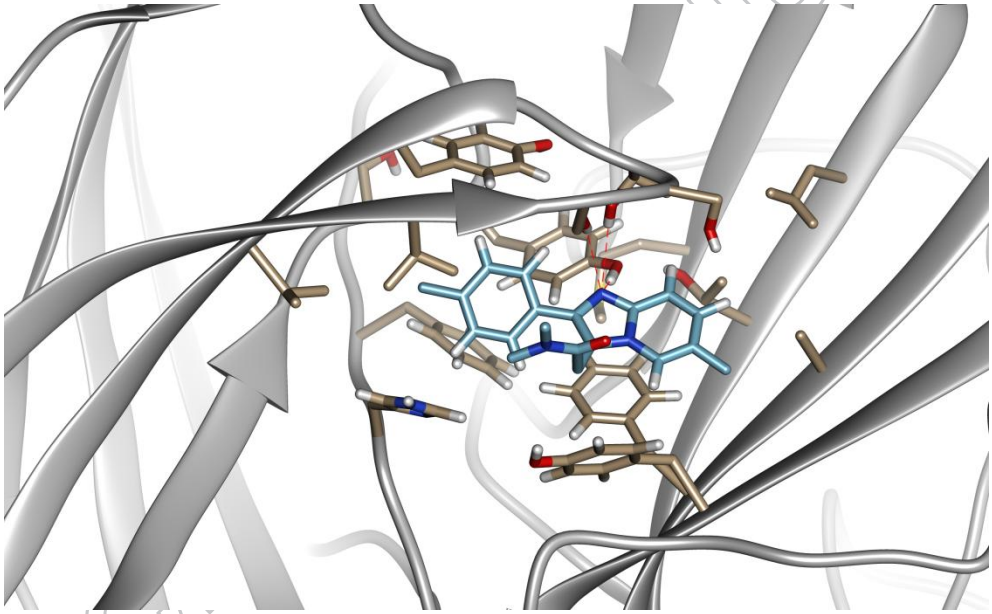

Figure S17. Zolpidem is depicted while bound to the modelled receptor in the middle frame of the clustering of the MD simulation.

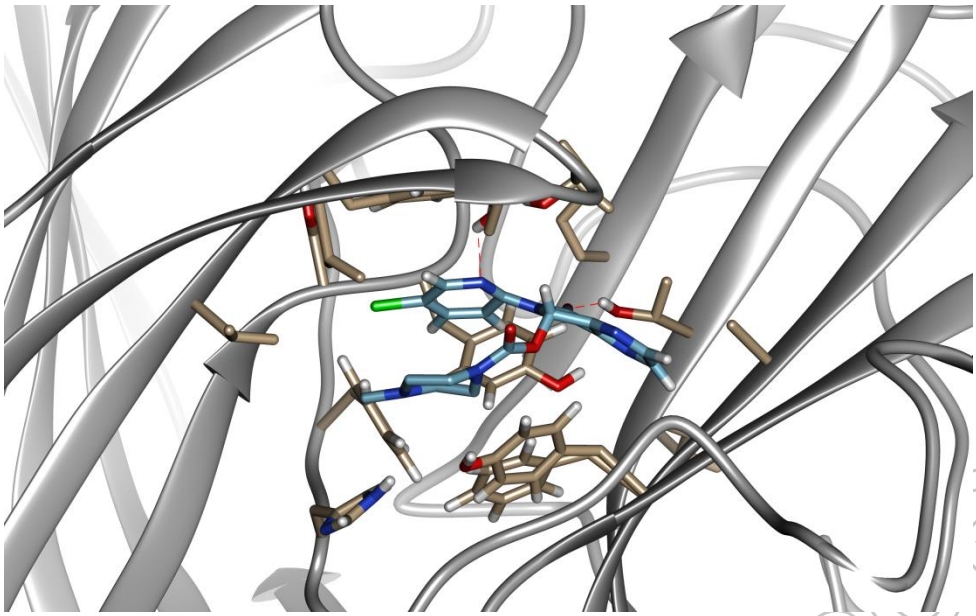

Figure S18. Eszopiclone is depicted while bound to the modelled receptor in the middle frame of the clustering of the MD simulation.

Behaviour observed in the simulations of GABA bound to $GABA_AR$.

It is interesting to highlight the behaviour, during the MD simulations of the holo-receptor with GABA bound, of certain residues, such as α_1Asp184, α_1Arg120, β_2Arg207, β_2Glu153 and β_2Glu155.

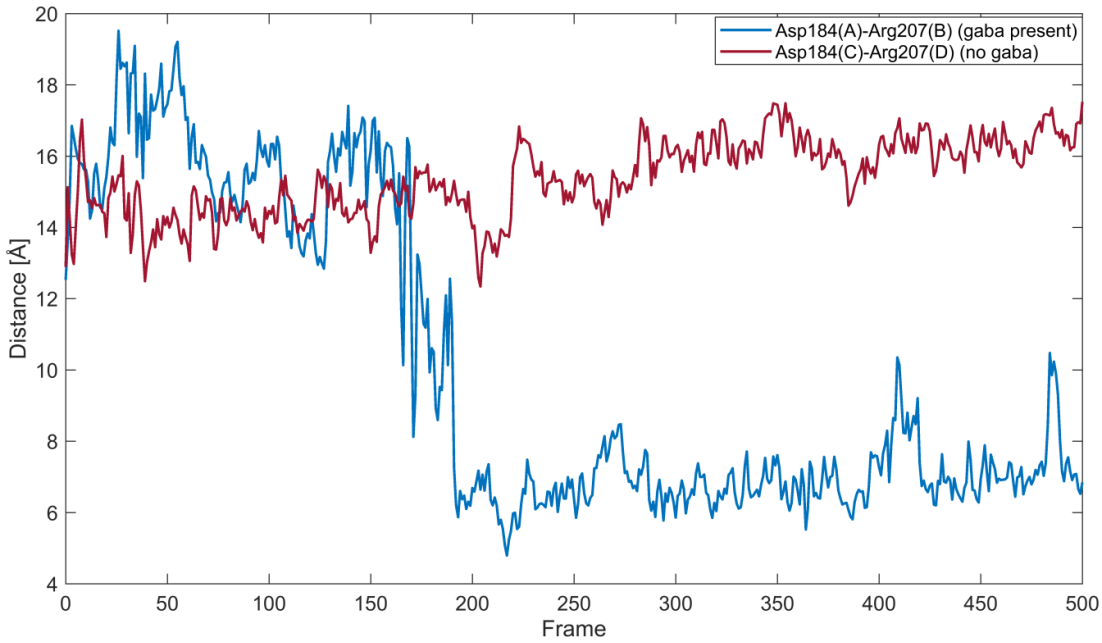

Figure S19. During the MD simulation of the receptor with a bound GABA molecule, we observed that Loop F approaches the principal face of the binding site. It is represented here as the distance between Asp184 of the aforementioned loop and Arg207 from loop C in the presence and absence of GABA.

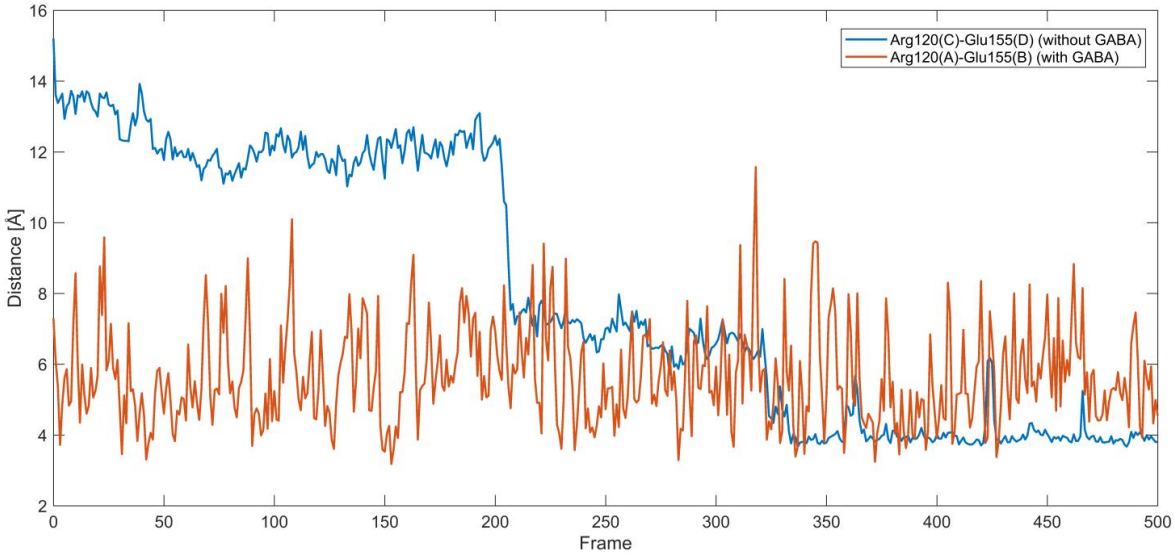

Figure S20. Interaction patterns for α_1Arg120 and β_2Glu155. The absence of GABA stabilizes the interaction between these two residues.

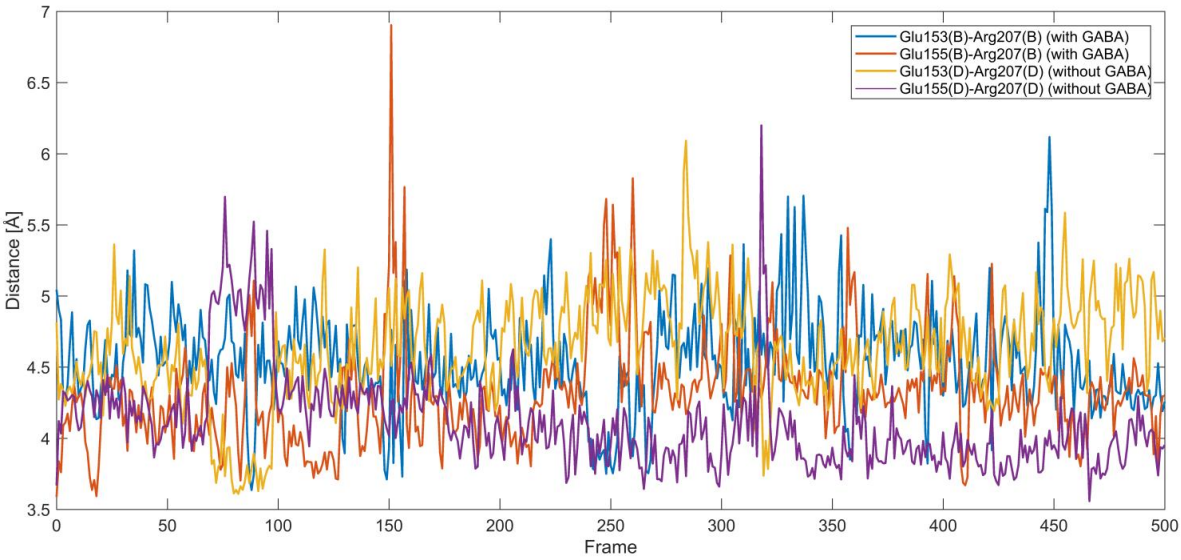

Figure S21. The interaction network of Glu153, Glu155 and Arg207 from the β_2 subunits does not display such noticeable differences in the presence/absence of GABA.

Interplay between experimental data and *in silico* predictions.

A drawback in contrasting experimental data with docking results lies in the fact that generally the former does not give accurate information about the actual interaction between the ligands and the amino acids. Through mutational studies, photolabelling, cysteine substitution methods, etc., amino acids which are somehow involved in the interaction or are part of the binding cavity can be detected. However this does not necessarily mean they are directly interacting with the compounds; they can instead have an active role in preserving the shape of the binding cavity or they might be forming networks of interactions with contacting residues and therefore mediating local conformational movements. Within this uncertainty we predicted the binding modes for the chosen ligands, knowing that in several circumstances

different orientations are possible within the binding cavity. In this regard, it has been proposed for PLGICs that the ligands might act as a wedge between residues in the binding site initiating the allosteric transmission of the signal, without engaging in precise interactions (Mu, Lester, & Dougherty, 2003).

Conventionally, docking protocols exhibit a weakness regarding the correct estimation of the binding affinities since the values are highly dependent on the scoring function employed (Kitchen, Decornez, Furr, & Bajorath, 2004; Lenselink et al., 2016; Olsson, García-Sosa, & Ryde, 2018). As a matter of fact, the software programs employed in this work offer different ways of calculating the probability of the binding pose. HADDOCK, for instance, does not deliver a value for energy of binding, but calculates and classifies the structures according to the HADDOCK score (Kastritis & Bonvin, 2010), which cannot be directly correlated to the energy of the binding. Moreover, although AutoDock Vina gives an energy value estimation, it is not directly comparable to experimental binding energies either (Ramírez & Caballero, 2016; Trott & Olson, 2010). We compared the energy of binding according to AutodockVina for the ligands of the orthosteric cavity to those measured experimentally (Table S8) and saw no correlation or trend in the results, consistently with the above cited references.

Table S8. The comparison of the values for the binding energy of different compounds of the orthosteric cavity constitutes a clear example of the limitation of the docking programs to correctly evaluate this function.

Ligand	**Experimental Ki [nmol]** (Svend Erik Westh-Hansen et al., 1997)	**Experimental ΔG [kcal/mol]†**	**In sílico ΔG [kcal/mol]**
Muscimol	11,0	-10,9	-5,6
GABA	56,0	-9,9	-4,8
Gabazine	10,0	-10,9	-8,1
Bicuculline	7300,0	-7,0	-10,2

† Calculated using the equation $K_i = e^{-\Delta G/RT}$

Other computational approaches exist which attempt to estimate the free energy of binding, such as Free Energy Perturbation, Linear Interaction Energy and MM-PBSA. However, these are very computationally expensive and in some cases are not accurate enough (Chipot, 2013; Gaieb et al., 2018).

Bearing this limitation in mind, we employed a different methodology for evaluating the docking poses; we contrasted the best binding modes according to each software against experimental information regarding the interactions with surrounding amino acids. This evaluation method has been successfully applied in similar works (Fierro, Suku, Alfonso-prieto, & Giorgetti, 2017; Sandal et al., 2015).

References

Alonso, H., Bliznyuk, A. A., & Gready, J. E. (2006). Combining Docking and Molecular Dynamic Simulations in Drug Design. *Medicinal Research Reviews*, *26*(5), 531–568. http://doi.org/10.1002/med.20067

Amin, J., Brooks-Kayal, A. M. Y., & Weiss, D. S. (1997). Two tyrosine residues on the α subunit are crucial for benzodiazepine binding and allosteric modulation of γ-aminobutyric acidA receptors. *Molecular Pharmacology*, *51*(5), 833–841. http://doi.org/10.1124/mol.51.5.833

Amin, J., & Weiss, D. S. (1993). GABAA receptor needs two homologous domains of the beta-subunit for activation by GABA but not by pentobarbital. *Nature*, *366*(6455), 565--569. http://doi.org/10.1038/366565a0

Benson, J. A., Löw, K., Keist, R., Mohler, H., & Rudolph, U. (1998). Pharmacology of recombinant gamma-aminobutyric acid A receptors rendered diazepam-insensitive by point-mutated alpha-subunits. *FEBS Letters*, *431*, 400–404. http://doi.org/10.1016/S0014-5793(98)00803-5

Berezhnoy, D., Nyfeler, Y., Gonthier, A., Goeldner, M., & Sigel, E. (2004). On the Benzodiazepine Binding Pocket in GABA A Receptors. *Biochemistry*, *279*(5), 3160–3168. http://doi.org/10.1074/jbc.M311371200

Bergmann, R., Kongsbak, K., Sørensen, P. L., Sander, T., & Balle, T. (2013). A Unified Model of the GABAA Receptor Comprising Agonist and Benzodiazepine Binding Sites. *PLoS ONE*, *8*(1), 1–13. http://doi.org/10.1371/journal.pone.0052323

Boileau, A. J., Evers, A. R., Davis, A. F., & Czajkowski, C. (1999). Mapping the Agonist Binding Site of the GABAAReceptor: Evidence for a β-Strand. *Journal of Neuroscience*, *19*(12), 4847–4854. Retrieved from http://www.jneurosci.org/content/19/12/4847

Boileau, A. J., Newell, J. G., & Czajkowski, C. (2002). GABAA receptor beta2 Tyr97 and Leu99 line the GABA-binding site. Insights into mechanisms of agonist and antagonist actions.

Journal of Biological Chemistry, *277*(4), 2931–2937. http://doi.org/10.1074/jbc.M109334200

Bordogna, A., Pandini, A., & Bonati, L. (2011). Predicting the accuracy of protein–ligand docking on homology models. *Journal of Computational Chemistry*, *32*(1), 81–98. http://doi.org/10.1002/jcc.21601

Buhr, A., Baur, R., Malherbe, P., & Sigel, E. (1996). Point mutations of the alpha1 beta2 gamma2 gamma-aminobutyric acid(A) receptor affecting modulation of the channel by ligands of the benzodiazepine binding site. *Molecular Pharmacology*, *49*(6), 1080–1084.

Buhr, A., Baur, R., & Sigel, E. (1997). Subtle changes in residue 77 of the γ subunit of α1β2γ2 GABAA receptors drastically alter the affinity for ligands of the benzodiazepine binding site. *Journal of Biological Chemistry*, *272*(18), 11799–11804. http://doi.org/10.1074/jbc.272.18.11799

Buhr, A., Schaerer, M. T., Baur, R., & Sigel, E. (1997). Residues at positions 206 and 209 of the α1 subunit of γ-aminobutyric acidA receptors influence affinities for benzodiazepine binding site ligands. *Molecular Pharmacology*, *52*(4), 676–682. http://doi.org/10.1124/mol.52.4.676

Buhr, A., & Sigel, E. (1997). A point mutation in the γ2 subunit of γ-aminobutyric acid type A receptors results in altered benzodiazepine binding site specificity. *Proceedings of the National Academy of Sciences*, *94*(16), 8824–8829.

Chipot, C. (2013). Frontiers in free-energy calculations of biological systems, *0*, 1–19. http://doi.org/10.1002/wcms.1157

Davies, M., Newell, J. G., Derry, J. M. C., Martin, I. A. N. L., & Dunn, S. M. J. (2000). Characterization of the Interaction of Zopiclone with gamma-Aminobutyric Acid Type A Receptors. *Molecular Pharmacology*, *58*(4), 756–762. http://doi.org/10.1124/mol.58.4.756

Derry, J. M. C., Dunn, S. M. J., & Davies, M. (2004). Identification of a residue in the gamma-aminobutyric acid type A receptor a subunit that differentially affects diazepam-sensitive and -insensitive benzodiazepine site binding. *Journal of Neurochemistry*, *88*, 1431–1438. http://doi.org/10.1046/j.1471-4159.2003.02264.x

Duncalfe, L. L., Carpenter, M. R., Smillie, L. B., Martin, I. L., & Dunn, S. M. (1996). The major site

of photoaffinity labeling of the gamma-aminobutyric acid type A receptor by [3H]flunitrazepam is histidine 102 of the alpha subunit. *The Journal of Biological Chemistry*, *271*(16), 9209–9214. http://doi.org/10.1074/jbc.271.16.9209

Fierro, F., Suku, E., Alfonso-prieto, M., & Giorgetti, A. (2017). Agonist Binding to Chemosensory Receptors : A Systematic Bioinformatics Analysis. *Frontiers in Molecular Biosciences*, *4*(September), 1–14. http://doi.org/10.3389/fmolb.2017.00063

Gaieb, Z., Liu, S., Gathiaka, S., Chiu, M., Yang, H., Shao, C., … Amaro, R. E. (2018). D3R Grand Challenge 2: blind prediction of protein–ligand poses, affinity rankings, and relative binding free energies. *Journal of Computer-Aided Molecular Design*, *32*(1), 1–20. http://doi.org/10.1007/s10822-017-0088-4

Goldschen-Ohm, M., Wagner, D., & Jones, M. (2011). Three arginines in the GABAA receptor binding pocket have distinct roles in the formation and stability of agonist-versus antagonist-bound complexes. *Molecular Pharmacology*, *80*(4), 647–656. http://doi.org/10.1124/mol.111.072033.2002

Hanson, S. M., & Czajkowski, C. (2008). Structural mechanisms underlying benzodiazepine modulation of the GABA(A) receptor. *The Journal of Neuroscience*, *28*(13), 3490–9. http://doi.org/10.1523/JNEUROSCI.5727-07.2008

Hanson, S. M., Morlock, E. V., Satyshur, K. A., & Czajkowski, C. (2008). Structural Requirements for Eszopiclone and Zolpidem Binding to the γ-Aminobutyric Acid Type-A (GABAA) Receptor Are Different. *Journal of Medicinal Chemistry*, *51*(22), 7243–7252. http://doi.org/10.1021/jm800889m

Hilf, R. J. C., & Dutzler, R. (2008). X-ray structure of a prokaryotic pentameric ligand-gated ion channel. *Nature*, *452*(7185), 375–379. http://doi.org/10.1038/nature06717

Holden, J. H., & Czajkowski, C. (2002). Different residues in the GABAA receptor α1T60-α1K70 region mediate GABA and SR-95531 actions. *Journal of Biological Chemistry*, *277*(21), 18785–18792. http://doi.org/10.1074/jbc.M111778200

Kastritis, P. L., & Bonvin, A. M. J. J. (2010). Are Scoring Functions in Protein - Protein Docking Ready To Predict Interactomes? Clues from a Novel Binding Affinity Benchmark research articles. *Journal of Proteome Research*, *9*, 2216–2225.

Kitchen, D. B., Decornez, H., Furr, J. R., & Bajorath, J. (2004). DOCKING AND SCORING IN

VIRTUAL SCREENING FOR DRUG DISCOVERY : METHODS AND APPLICATIONS. *Nature Reviews*, *3*(November), 935–949. http://doi.org/10.1038/nrd1549

Kloda, J. H., & Czajkowski, C. (2007). Agonist-, Antagonist-, and Benzodiazepine-Induced Structural Changes in the alpha 1 Met 113 -Leu 132 Region of the GABA A Receptor. *Molecular Pharmacology*, *71*(2), 483–493. http://doi.org/10.1124/mol.106.028662.critical

Kucken, A. M., Teissére, J. a, Seffinga-clark, J., Wagner, D. a, & Czajkowski, C. (2003). Structural requirements for imidazobenzodiazepine binding to GABA(A) receptors. *Molecular Pharmacology*, *63*(2), 289–296. http://doi.org/10.1124/mol.63.2.289

Kucken, A. M., Wagner, D. A., Ward, P. R., Teissére, J. A., Boileau, A. J., & Czajkowski, C. (2000). Identification of Benzodiazepine Binding Site Residues in the gamma2 Subunit of the gamma-Aminobutyric Acid A Receptor. *Molecular Pharmacology*, *57*(5), 932–939.

Lenselink, E. B., Louvel, J., Forti, A. F., Veldhoven, J. P. D. Van, Vries, H. De, Mulder-krieger, T., … Beuming, T. (2016). Predicting Binding Affinities for GPCR Ligands Using Free-Energy Perturbation. *ACS Omega*, *1*(2), 293–304. http://doi.org/10.1021/acsomega.6b00086

Maggiora, G., Vogt, M., Stumpfe, D., & Bajorath, J. (2014). Molecular Similarity in Medicinal Chemistry. *Journal of Medicinal Chemistry*, *57*(8), 3186–3204. http://doi.org/10.1021/jm401411z

Middendorp, S. J., Hurni, E., Schönberger, M., Stein, M., Pangerl, M., Trauner, D., & Sigel, E. (2014). Relative positioning of classical benzodiazepines to the γ2-subunit of GABAA receptors. *ACS Chemical Biology*, *9*(8), 1846–1853. http://doi.org/10.1021/cb500186a

Mihic, S. J., Whiting, P. J., Klein, R. L., Wafford, K. A., & Harris, R. A. (1994). A single amino acid of the human gamma-aminobutyric acid type A receptor gamma 2 subunit determines benzodiazepine efficacy. *The Journal of Biological Chemistry*, *269*(52), 32768–73. Retrieved from http://www.ncbi.nlm.nih.gov/pubmed/7806498

Miller, P. S., & Aricescu, A. R. (2015). Crystal structure of a human GABAA receptor. *Nature*, *512*(7514), 270–275. http://doi.org/10.1038/nature13293

Morlock, E. V, & Czajkowski, C. (2011). Different residues in the GABAA receptor benzodiazepine binding pocket mediate benzodiazepine efficacy and binding. *Mol Pharmacol*, *80*(1), 14–22. http://doi.org/10.1124/mol.110.069542

Mu, T., Lester, H. A., & Dougherty, D. A. (2003). Different Binding Orientations for the Same Agonist at Homologous Receptors: A Lock and Key or a Simple Wedge? *Journal of the American Chemical Society*, *125*(23), 6850–6851. http://doi.org/10.1021/ja0348086

Newell, J. G., & Czajkowski, C. (2003). The GABAA receptor Alpha1 subunit Pro174-Asp191 segment is involved in GABA binding and channel gating. *Journal of Biological Chemistry*, *278*(15), 13166–13172. http://doi.org/10.1074/jbc.M211905200

Newell, J. G., McDevitt, R. A., & Czajkowski, C. (2004). Mutation of glutamate 155 of the GABAA receptor β2 subunit produces a spontaneously open channel: a trigger for channel activation. *Journal of Neuroscience*, *24*(50), 11226–11235. http://doi.org/10.1523/JNEUROSCI.3746-04.2004

Olsson, M. A., García-Sosa, A. T., & Ryde, U. (2018). Binding affinities of the farnesoid X receptor in the D3R Grand Challenge 2 estimated by free-energy perturbation and docking. *Journal of Computer-Aided Molecular Design*, *32*(1), 211–224. http://doi.org/10.1007/s10822-017-0056-z

Padgett, C. L., Hanek, A. P., Lester, H. A., Dougherty, D. A., & Lummis, S. C. R. (2007). Unnatural Amino Acid Mutagenesis of the GABAA Receptor Binding Site Residues Reveals a Novel Cation- Interaction between GABA and 2Tyr97. *Journal of Neuroscience*, *27*(4), 886–892. http://doi.org/10.1523/JNEUROSCI.4791-06.2007

Pritchett, D. B., & Seeburg, P. H. (1991). gamma-Aminobutyric acid type A receptor point mutation increases the affinity of compounds for the benzodiazepine site. *Proceedings of the National Academy of Sciences*, *88*(4), 1421–1425.

Ramírez, D., & Caballero, J. (2016). Is It Reliable to Use Common Molecular Docking Methods for Comparing the Binding Affinities of Enantiomer Pairs for Their Protein Target ? *International Journal of Molecular Sciences*, *17*(525), 1–15. http://doi.org/10.3390/ijms17040525

Rodrigues, J. P. G. L. M., Melquiond, A. S. J., Karaca, E., Trellet, M., van Dijk, M., van Zundert, G. C. P., … Bonvin, A. M. J. J. (2013). Defining the limits of homology modeling in information-driven protein docking. *Proteins: Structure, Function, and Bioinformatics*, *81*(12), 2119–2128. http://doi.org/10.1002/prot.24382

Sandal, M., Behrens, M., Brockhoff, A., Musiani, F., Carloni, P., & Meyerhof, W. (2015). Evidence for a Transient Additional Ligand Binding Site in the TAS2R46 Bitter Taste

Receptor. *Journal of Chemical Theory and Computation*, *11*(9), 4439–4449. http://doi.org/10.1021/acs.jctc.5b00472

Sawyer, G. W., Chiara, D. C., Olsen, R. W., & Cohen, J. B. (2002). Identification of the Bovine γ-Aminobutyric Acid Type A Receptor α Subunit Residues Photolabeled by the Imidazobenzodiazepine [3H] Ro15-4513. *Journal of Biological Chemistry*, *277*(51), 50036–50045. http://doi.org/10.1074/jbc.M209281200

Schaerer, M. T., Buhr, A., Baur, R., & Sigel, E. (1998). Amino acid residue 200 on the alpha1 subunit of GABA A receptors affects the interaction with selected benzodiazepine binding site ligands. *European Journal of Pharmacology*, *354*, 283–287. http://doi.org/10.1016/S0014-2999(98)00456-7

Sigel, E., Baur, R., Kellenberger, S., & Malherbe, P. (1992). Point mutations affecting antagonist affinity and agonist dependent gating of GABAA receptor channels. *The EMBO Journal*, *1*(6), 2017–2023.

Sigel, E., Schaerer, M. T., Buhr, A., & Baur, R. (1998). The Benzodiazepine Binding Pocket of Recombinant alpha1 beta2 gamma2 gamma-Aminobutyric Acid A Receptors: Relative Orientation of Ligands and Amino Acid Side Chains. *Molecular Pharmacology*, *54*(6), 1097–1105. http://doi.org/10.1124/mol.54.6.1097

Smart, O. S., Neduvelil, J. G., Wang, X., Wallace, B. A., & Sansom, M. S. P. (1996). HOLE: a program for the analysis of the pore dimensions of ion channel structural models. *Journal of Molecular Graphics*, *14*(6), 354–360. http://doi.org/10.1016/S0263-7855(97)00009-X

Smith, G. B., & Olsen, R. W. (1994). Identification of a [3H] muscimol photoaffinity substrate in the bovine gamma-aminobutyric acidA receptor alpha subunit. *Journal of Biological Chemistry*, *269*(32), 20380–20387.

Tan, K. R., Baur, R., Charon, S., Goeldner, M., & Sigel, E. (2009). Relative positioning of diazepam in the benzodiazepine-binding-pocket of GABAA receptors. *Journal of Neurochemistry*, *111*(5), 1264–1273. http://doi.org/10.1111/j.1471-4159.2009.06419.x

Tan, K. R., Baur, R., Gonthier, A., Goeldner, M., & Sigel, E. (2007). Two neighboring residues of loop A of the alpha1 subunit point towards the benzodiazepine binding site of GABAA receptors. *FEBS Letters*, *581*(24), 4718–4722. http://doi.org/10.1016/j.febslet.2007.08.068

Tan, K. R., Gonthier, A., Baur, R., Ernst, M., Goeldner, M., & Sigel, E. (2007). Proximity-accelerated chemical coupling reaction in the benzodiazepine-binding site of γ-aminobutyric acid type A receptors: Superposition of different allosteric modulators. *Journal of Biological Chemistry*, *282*(36), 26316–26325. http://doi.org/10.1074/jbc.M702153200

Teissére, J. A., & Czajkowski, C. (2001). A (beta)-strand in the (gamma)2 subunit lines the benzodiazepine binding site of the GABA A receptor: structural rearrangements detected during channel gating. *The Journal of Neuroscience : The Official Journal of the Society for Neuroscience*, *21*(14), 4977–4986. Retrieved from http://www.ncbi.nlm.nih.gov/pubmed/11438573

Trott, O., & Olson, A. J. (2010). AutoDock Vina: Improving the speed and accuracy of docking with a new scoring function, efficient optimization, and multithreading. *Journal of Computational Chemistry*, *31*(2), 455–461. http://doi.org/10.1002/jcc.21334

Unwin, N. (2005). Refined structure of the nicotinic acetylcholine receptor at 4 Å resolution. *Journal of Molecular Biology*, *346*(4), 967–989. http://doi.org/10.1016/j.jmb.2004.12.031

Wagner, D. A., & Czajkowski, C. (2001). Structure and dynamics of the GABA binding pocket: A narrowing cleft that constricts during activation. *The Journal of Neuroscience*, *21*(1), 67–74.

Wagner, D. A., Czajkowski, C., & Jones, M. V. (2004). An Arginine Involved in GABA Binding and Unbinding But Not Gating of the GABAA Receptor. *Journal of Neuroscience*, *24*(11), 2733–2741. http://doi.org/10.1523/JNEUROSCI.4316-03.2004

Westh-Hansen, S. E., Rasmussen, P. B., Hastrup, S., Nabekura, J., Noguchi, K., Akaike, N., … Nielsen, M. (1997). Decreased agonist sensitivity of human GABA A receptors by an amino acid variant, isoleucine to valine, in the alpha1 subunit. *European Journal of Pharmacology*, *329*(2–3), 253–257. http://doi.org/10.1016/S0014-2999(97)89186-8

Westh-Hansen, S. E., Witt, M. R., Dekermendjian, K., Liljefors, T., Rasmussen, P. B. ., & Nielsen, M. (1999). Arginine residue 120 of the human GABA A receptor alpha 1 , subunit is essential for GABA binding and chloride ion current gating. *Neuropharmacology*, *10*(11), 2417–2421.

Wieland, H. A., & Lüddens, H. (1994). Four Amino Acid Exchanges Convert a Diazepam-Insensitive, Inverse Agonist-Preferring GABAA Receptor into a Diazepam-Preferring

GABAA Receptor. *Journal of Medicinal Chemistry*, *37*(26), 4576–4580. http://doi.org/10.1021/jm00052a019

Wieland, H. A., Lüddens, H., & Seeburg, P. H. (1992). A single histidine in GABAA receptors is essential for benzodiazepine agonist binding. *Journal of Biological Chemistry*, *267*(3), 1426–1429. http://doi.org/VL - 267

Wingrove, P. B., Thompson, S. A., Wafford, K. A., & Whiting, P. J. (1997). Key Amino Acids in the γ Subunit of the γ-Aminobutyric Acid A Receptor that Determine Ligand Binding and Modulation at the Benzodiazepine Site. *Molecular Pharmacology*, *52*(5), 874 LP-881. Retrieved from http://molpharm.aspetjournals.org/content/52/5/874.abstract